

# Accepted Manuscript

Design and development of novel *N*-(pyrimidin-2-yl)-1,3,4-oxadiazole hybrids to treat cognitive dysfunctions

Prabhash Nath Tripathi, Pavan Srivastava, Piyooosh Sharma, Ankit Seth, Sushant K. Shrivastava

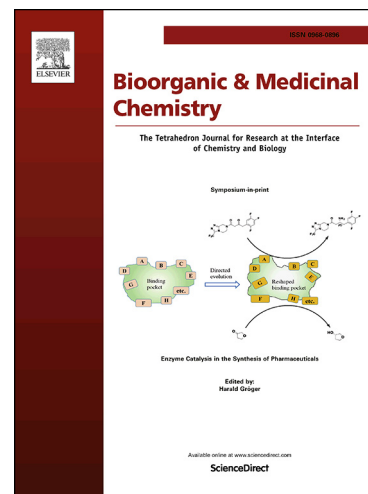
PII: S0968-0896(18)31848-0  
DOI: <https://doi.org/10.1016/j.bmc.2019.02.031>  
Reference: BMC 14767

To appear in: *Bioorganic & Medicinal Chemistry*

Received Date: 3 November 2018  
Revised Date: 14 February 2019  
Accepted Date: 15 February 2019

Please cite this article as: Tripathi, P.N., Srivastava, P., Sharma, P., Seth, A., Shrivastava, S.K., Design and development of novel *N*-(pyrimidin-2-yl)-1,3,4-oxadiazole hybrids to treat cognitive dysfunctions, *Bioorganic & Medicinal Chemistry* (2019), doi: <https://doi.org/10.1016/j.bmc.2019.02.031>

This is a PDF file of an unedited manuscript that has been accepted for publication. As a service to our customers we are providing this early version of the manuscript. The manuscript will undergo copyediting, typesetting, and review of the resulting proof before it is published in its final form. Please note that during the production process errors may be discovered which could affect the content, and all legal disclaimers that apply to the journal pertain.



**Design and development of novel *N*-(pyrimidin-2-yl)-1,3,4-oxadiazole hybrids to treat cognitive dysfunctions**

Prabhash Nath Tripathi, Pavan Srivastava, Piyoosh Sharma, Ankit Seth, Sushant K. Shrivastava\*

*Pharmaceutical Chemistry Research Laboratory, Department of Pharmaceutical Engineering & Technology, Indian Institute of Technology (Banaras Hindu University), Varanasi – 221 005 (India)*

\*Address correspondence to:

**Dr. Sushant Kumar Shrivastava**

Professor

Department of Pharmaceutical Engineering & Technology,

Indian Institute of Technology

(Banaras Hindu University), Varanasi- 221 005, India

Email: skshrivastava.phe@itbhu.ac.in

Phone: +91-542-6702725

**ABSTRACT**

Novel hybrids bearing a 2-aminopyrimidine (2-AP) moiety linked to substituted 1,3,4-oxadiazoles were designed, synthesized and biologically evaluated. Among the developed compounds, **28** noncompetitively inhibited human acetylcholinesterase (hAChE;  $pIC_{50} = 6.52$ ;  $K_i = 0.17 \mu M$ ) and showed potential *in vitro* antioxidant activity (60.0%) when evaluated using the Ellman's and DPPH assays, respectively. Compound **28** competitively displaced propidium iodide (PI) from the peripheral anionic site (PAS) of hAChE (17.6%) and showed high blood-brain barrier (BBB) permeability, as observed in the PAMPA-BBB assay. Additionally, compound **28** inhibited hAChE-induced A $\beta$  aggregation in a concentration-dependent manner according to the thioflavin T assay and was devoid of neurotoxic liability towards SH-SY5Y cell lines, as demonstrated by the MTT assay. The behavioral studies of compound **28** in mice showed a significant reversal of scopolamine-induced amnesia, as observed in Y-maze and passive avoidance tests. Furthermore, compound **28** exhibited significant AChE inhibition in the brain in *ex vivo* studies. An evaluation of oxidative stress biomarkers revealed the antioxidant potential of **28**. Moreover, *in silico* molecular docking and dynamics simulation studies were used as a computational tool to evaluate the interactions of compound **28** with the active site residues of hAChE.

**Keywords:** Acetylcholinesterase; A $\beta$  aggregation; Antioxidant; 2-Aminopyrimidine; 1,3,4-Oxadiazole.

## 1. INTRODUCTION

Cognition is a combination of attention, perception, acquaintance, skills, memory, reminiscence, decision making, planning and judgment that define the normal nature of human beings.<sup>1,2</sup> Memory loss and cognitive impairment are observed in various conditions, such as aging,<sup>3</sup> stroke,<sup>4</sup> toxicant exposure,<sup>5</sup> head injury<sup>6</sup> and neurodegenerative disorders such as schizophrenia, depression, Alzheimer's disease (AD)<sup>7,8</sup> and Parkinson's disease.<sup>9,10</sup> Neurotransmitters such as acetylcholine (ACh),<sup>11</sup> dopamine,<sup>12</sup> serotonin,<sup>13</sup> and glutamate<sup>14</sup> are responsible for regulating cognitive functions. Among these compounds, ACh, which is hydrolyzed by acetylcholinesterase (AChE) into choline and acetic acid,<sup>15</sup> is an important neurotransmitter in the regulation of learning and memory processes. Low levels of ACh in the hippocampus, cortex area and basal forebrain have been implicated in cognitive deficit and loss of short-term memory.<sup>16,17</sup> AChE also induces the aggregation and deposition of A $\beta$  fibrils by forming AChE-A $\beta$  complexes, leading to cognitive dysfunction.<sup>18,19</sup> Hence, the elevation of ACh through AChE inhibition and the prevention of A $\beta$  aggregation are the two most promising approaches to halting the progression of dementia. Additionally, oxidative stress is another damaging factor caused by an imbalance between the generation of reactive oxygen species (ROS) and antioxidant enzymes. Excessive ROS release triggers protein oxidation and lipid peroxidation, which subsequently cause oxidative damage and lead to impaired cognitive function. Research also suggests that A $\beta$  could enter the mitochondria, increasing the generation of free radicals and inducing oxidative stress.<sup>20-22</sup>

Currently, there are three AChE inhibitors (donepezil, rivastigmine and galantamine) approved by the US FDA to relieve the symptoms of AD, but these compounds have no active role in the prevention of disease progression.<sup>23</sup> These drugs exhibit several side effects, such as urinary incontinence, weakness and muscle cramps, which limits their use in the advanced stages of the disease.<sup>24,25</sup> Therefore, the development of novel neuro-therapeutic

agents that will impede the metabolism of ACh by inhibiting AChE and preventing A $\beta$  aggregation and provide antioxidant activity to decelerate disease progression is of great importance.<sup>26</sup>

### 1.1. Designing Considerations

These molecules were designed based on the bioisosteric replacement and hybrid pharmacophore approach. Several pyrimidine-based derivatives have been explored as attractive scaffolds because of their broad biological activities.<sup>27-30</sup> Derivatives containing pyrimidine-fused heterocyclic rings, such as sugar-linked 2-oxo- and 2-thioxo-pyrimidine, 5*H*-thiazolo[3,2-*a*]pyrimidine, pyrimidine-triazolopyrimidine, pyrimidine-pyridine and thiazolo-pyrimidine hybrids (**I**), have been reported to show AChE inhibitory activity.<sup>31-33</sup> These studies have suggested that 2*H*-thiazolo-[3,2-*a*]pyrimidine derivatives have a significant binding affinity towards AChE.<sup>34</sup> Furthermore, a [1,2,4]triazolo[1,5-*a*]pyrimidine derivative (**II**) was designed as a multifunctional agent capable of inhibiting AChE and AChE-induced A $\beta$  aggregation along with showing antioxidant activity.<sup>35</sup> A recent study also indicated that 4,6-diarylpyrimidine derivative **III** exhibited dual inhibitory activities against AChE and monoamine oxidase.<sup>36</sup> Additionally, a 2,4-disubstituted pyrimidine derivative (**IV**) has been reported to show cholinesterase (ChE) inhibitory and A $\beta$  anti-aggregatory activity.<sup>37-40</sup> On the basis of these reports, a 2-aminopyrimidine (2-AP) scaffold was selected and utilized as a template to design small molecules as potential therapeutics for the treatment of cognitive dysfunctions.

A series of heteroaromatic/aromatic ring-containing compounds, such as imidazole, acridine, cinnamide-dibenzylamine, *p*-aminobenzoic acid, triazine, and benzoxazole derivatives, were developed to evaluate their AChE/BChE inhibitory potential and their antioxidant activities for the treatment of dementia.<sup>7,8,10,41-43</sup> Compounds bearing a 1,3,4-oxadiazole nucleus have been reported to have various therapeutic applications in the field of drug discovery owing to

their planer aromatic core and ability to accept hydrogen bonds, which allow them to achieve the requisite orientation of their substituents within the enzyme pocket.<sup>44-46</sup> Additionally, compounds containing the 2,5-substituted-1,3,4-oxadiazole nucleus, such as 2-(furan-2-yl)-5-(3,4,5-trimethoxystyryl)-1,3,4-oxadiazole (**V**), 2-(2-(benzo[d][1,3]dioxol-5-yl)vinyl)-5-(2-chloro-4-fluorophenyl)-1,3,4-oxadiazole (**VI**) and 2-((benzothiazol-2-ylthio)methyl)-5-((4-bromobenzyl)thio)-1,3,4-oxadiazole (**VII**), significantly inhibit AChE and AChE-induced A $\beta$  aggregation and show neuroprotective activity.<sup>47-49</sup>

Considering the reported literature, the 2-AP moiety was tethered to a substituted 1,3,4-oxadiazole nucleus within a single hybrid pharmacophore skeleton with the aim of developing multitargeted ligands with the ability to inhibit AChE and AChE-induced A $\beta$  aggregation and serve as an antioxidant (Fig. 1).

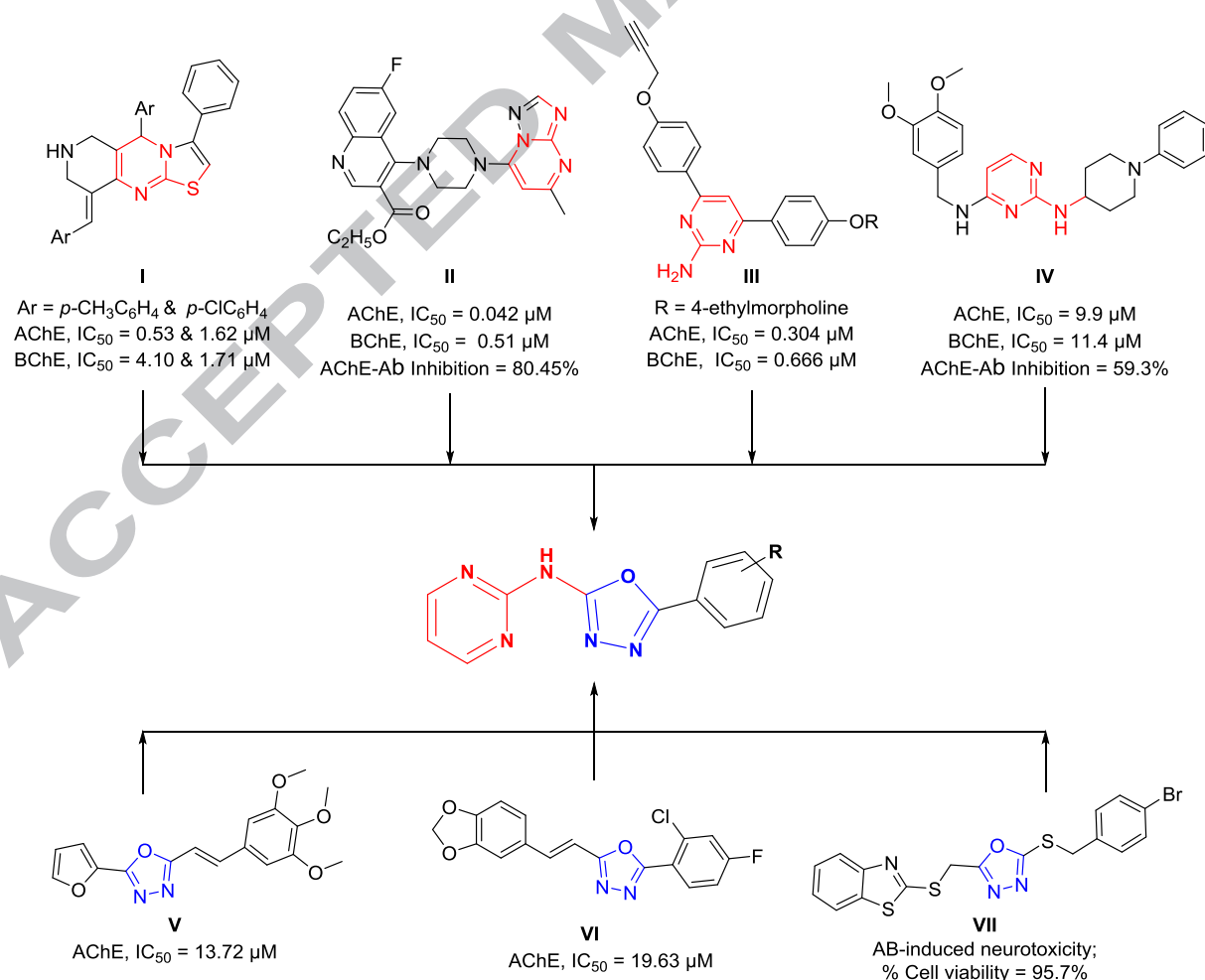


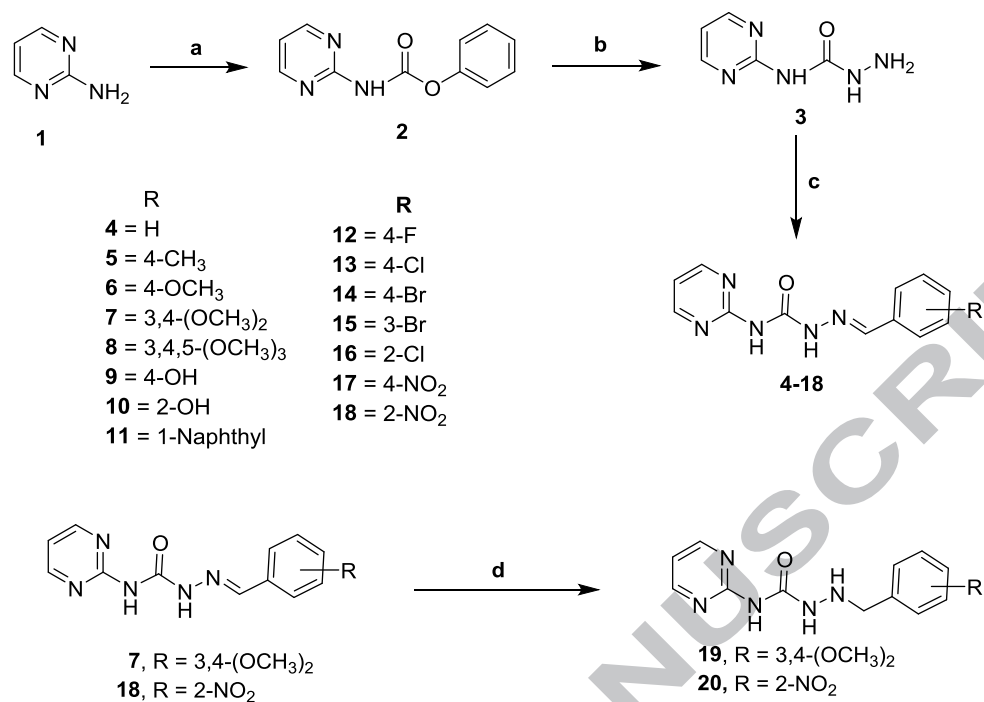
**Fig. 1.** Designing strategy for the target compounds.

## 2. RESULTS AND DISCUSSION

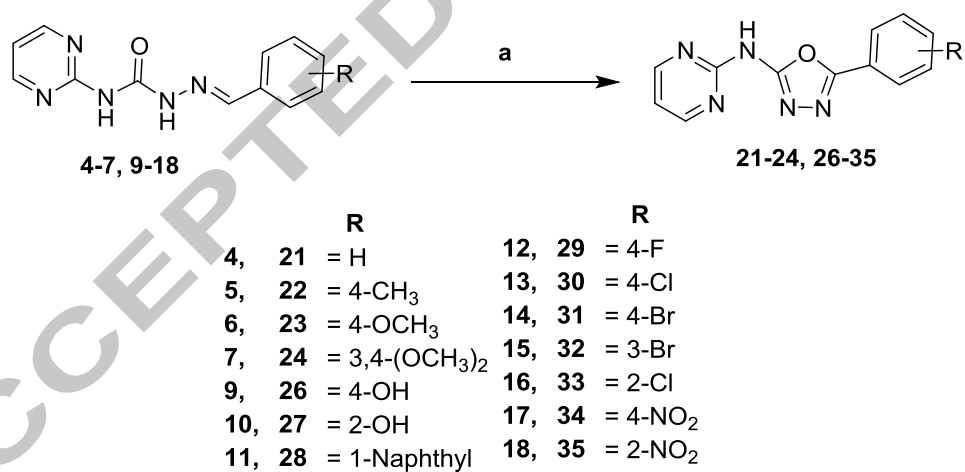
### 2.1. Chemistry

The title compounds (**4-20**) were prepared using the reaction sequence described in **Scheme 1**. In the first step, 2-AP (**1**) was reacted with phenyl chloroformate (PCF) and pyridine in dry dichloromethane (DCM) to yield phenyl pyrimidin-2-ylcarbamate (**2**). Key intermediate **3** was synthesized in an appreciable yield (81%) by refluxing compound **2** with hydrazine hydrate (85% v/v) in absolute ethanol. The subsequent reaction of compound **3** with numerous aromatic aldehydes in absolute ethanol yielded the corresponding semicarbazones (**4-18**). The reduction of compounds **4-18** was attempted with various reducing reagents, such as sodium cyanoborohydride ( $\text{NaBH}_3\text{CN}$ ), sodium triacetoxyborohydride ( $\text{NaBH}(\text{OAc})_3$ ), sodium borohydride-nickel chloride and sodium borohydride-cobalt chloride. However, only compounds **7** and **18** reacted with sodium borohydride ( $\text{NaBH}_4$ )<sup>50</sup> in dry methanol to afford their reduced congeners (**19** and **20**, respectively).

As shown in **Scheme 2**, compounds **4-7** and **9-18** were reacted with chloramine-T (CAT) in absolute ethanol to obtain the corresponding 1,3,4-oxadiazole derivatives (**21-24** and **26-35**) through an oxidative cyclization reaction. Compound **8** was cyclized using *N*-bromosuccinimide (NBS) and 1,8-diazabicyclo[5.4.0]undec-7-ene (DBU) as a base to afford compound **25**. All the synthesized compounds were preliminarily identified using Dragendorff's reagent on TLC (thin-layer chromatography).<sup>51</sup> The crude products were recrystallized from absolute ethanol to yield the title compounds. The structures of the compounds were confirmed by spectroscopic (FT-IR, <sup>1</sup>H NMR and <sup>13</sup>C NMR) and elemental analyses.



**Scheme 1.** Reagents and conditions: (a) PCF, pyridine, dry DCM, under nitrogen, 0-5 °C, 3 h; (b) 85% v/v hydrazine hydrate, absolute ethanol, reflux, 30 min; (c) various aromatic aldehydes, absolute ethanol, reflux, 3 h; (d) sodium borohydride, dry methanol, 0-5 °C, 1 h.



**Scheme 2.** Reagents and conditions: (a) CAT, absolute ethanol, reflux, 2 h; (b) NBS, DBU, dry DCM, room temperature, 3-4 h.

The  $^1\text{H}$  NMR spectrum confirmed the formation of compound **2**, as evidenced by the appearance of a carbamate proton peak at 11.31 ppm. The diagnostic peaks of the hydrazinecarboxamide ( $-\text{NHCONHNH}_2$ ) group of compound **3** appeared at 9.87, 9.65 and 4.24 ppm, respectively. Furthermore, the spectra of the semicarbazone derivatives (**4-18**) indicated the presence of a distinctive imine proton ( $-\text{HC}=\text{N}$ ) at 8.55-8.21 ppm, and the amine ( $-\text{NH}_2$ ) peak had disappeared. Additionally, the  $-\text{NHCONHN}=\text{CH}$  group exhibited two broad singlets between 12.55-12.23 ppm and 10.29-10.02 ppm, respectively. The 4-methyl ( $-\text{CH}_3$ ), 4-methoxy ( $-\text{OCH}_3$ ) and 3,4-dimethoxy ( $-\text{OCH}_3 \times 2$ ) groups in compounds **5**, **6** and **7** displayed characteristic signals at 2.34, 3.73 and 3.82 ppm, respectively. The three methoxy groups ( $-\text{OCH}_3 \times 3$ ) of compound **8** exhibited two singlet peaks for six protons and for three protons at 3.82 and 3.69 ppm, respectively. The formation of the 1,3,4-oxadiazole moiety in compounds **21-35** was confirmed by the absence of the distinctive peak of the imine proton.

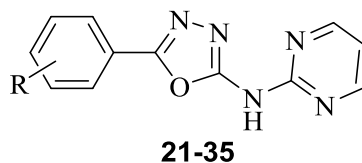
In their  $^{13}\text{C}$  NMR spectra, compounds **4-18**, with imine ( $-\text{N}=\text{CH}$ ) and carbonyl ( $-\text{NH}-\text{CO}-\text{NH}-$ ) groups, showed signals at approximately 151.3 ppm and 158.1 ppm, respectively. Compounds **5**, **6** and **7**, bearing 4-methyl, 4-methoxy and 3,4-dimethoxy groups, respectively, exhibited diagnostic signals at 21.4, 55.7 and 56.0 ppm. The methoxy carbons of the 3,4,5-trimethoxyphenyl group in compound **8** appeared as two signals at 60.5 and 56.3 ppm. The absence of the imine ( $-\text{N}=\text{CH}$ ) and carbonyl ( $>\text{C}=\text{O}$ ) signals in the spectra of compounds **4-18** and the subsequent appearance of ( $>\text{C}=\text{N}$ ) signals in the spectra of **21-35** confirmed the formation of a 1,3,4-oxadiazole ring. The purity of each intermediate and target compound was ascertained using elemental analysis, and the results were within  $\pm 0.4\%$  of the theoretical values.

## 2.2. Pharmacology

### 2.2.1. *In vitro* cholinesterase inhibition assay

All the synthesized compounds (**21-35**) were evaluated by Ellman's colorimetric method on hAChE (acetylcholinesterase from human erythrocyte) and hBChE (butyrylcholinesterase from human serum) using donepezil as a reference standard (Table 1). With the exceptions of compounds **27**, **33** and **34**, compounds **21-35** inhibited hAChE ( $pIC_{50} < 5.3$ ). Compound **21**, with a phenyl ring at the 5 position of the 1,3,4-oxadiazole core, exhibited considerable hAChE inhibitory activity ( $pIC_{50} = 5.69 \pm 0.02$ ). Among derivatives **22-27**, compound **25**, bearing an electron-donating 3,4,5-trimethoxyphenyl group, showed significant hAChE inhibitory potential ( $pIC_{50} = 5.91 \pm 0.11$ ). Next, of the compounds in this series, **29-35**, which possess electron-withdrawing groups on the phenyl ring, exhibited slightly diminished hAChE inhibitory activities compared to those of compounds **22-27**, which possess electron-donating groups. Among all the evaluated derivatives (**21-35**), compound **28**, bearing a naphthyl ring, displayed the most significant hAChE inhibitory activity ( $pIC_{50} = 6.52 \pm 0.04$ ). The enhanced lipophilicity of compound **28** due to its naphthyl group may be the cause of its effective interactions with the active site residues of hAChE. Compounds **28**, **31** and **32** were the only synthesized compounds that significantly inhibited hBChE.

**Table 1.** The results of the human cholinesterase (hAChE and hBChE) and DPPH assays of target compounds **21-35**.



Comp. Code	R	<sup>a</sup> pIC <sub>50</sub> ± SD		<sup>b</sup> SI	Reduction % DPPH at 20 μM
		hAChE	hBChE		
<b>21</b>	-H	5.69 ± 0.02	< 4.3	-	51.4 ± 1.7
<b>22</b>	4-CH <sub>3</sub>	5.79 ± 0.05	< 4.3	-	< 20
<b>23</b>	4-OCH <sub>3</sub>	5.81 ± 0.03	< 4.3	-	45.8 ± 2.7
<b>24</b>	3,4-(OCH <sub>3</sub> ) <sub>2</sub>	5.72 ± 0.12	< 4.3	-	49.5 ± 2.4
<b>25</b>	3,4,5-(OCH <sub>3</sub> ) <sub>3</sub>	5.91 ± 0.11	< 4.3	-	57.7 ± 4.4
<b>26</b>	4-OH	5.76 ± 0.06	< 4.3	-	63.4 ± 1.9
<b>27</b>	2-OH	< 5.3	< 4.3	-	58.8 ± 1.9
<b>28</b>	1-Naphthyl	6.52 ± 0.04	4.92 ± 0.05	39.81	60.0 ± 2.3
<b>29</b>	4-F	5.62 ± 0.05	< 4.3	-	41.9 ± 1.1
<b>30</b>	4-Cl	5.54 ± 0.03	< 4.3	-	46.2 ± 2.1
<b>31</b>	4-Br	5.43 ± 0.03	4.64 ± 0.07	6.17	47.8 ± 1.7
<b>32</b>	3-Br	5.48 ± 0.15	4.69 ± 0.04	6.17	47.9 ± 2.6
<b>33</b>	2-Cl	< 5.3	< 4.3	-	< 20
<b>34</b>	4-NO <sub>2</sub>	< 5.3	< 4.3	-	< 20
<b>35</b>	2-NO <sub>2</sub>	5.47 ± 0.04	< 4.3	-	51.8 ± 3.3
donepezil	-	6.83 ± 0.02	5.32 ± 0.04	32.36	< 20
ascorbic acid	-	-	-	-	64.6 ± 5.8

All the values are expressed as the mean ± S.D. (n=3); <sup>a</sup>pIC<sub>50</sub> = [-Log (IC<sub>50</sub> × 10<sup>-6</sup> M)]; <sup>b</sup>selectivity index (S.I.) corresponds to the antilog of ΔpIC<sub>50</sub>; (ΔpIC<sub>50</sub> = pIC<sub>50</sub> hAChE - pIC<sub>50</sub> hBChE).<sup>52</sup>

### 2.2.2 hAChE kinetics study with compound 28

Compound **28** was subjected to an enzyme kinetics study to determine the type of hAChE inhibition using a Lineweaver-Burk plot (1/V<sub>max</sub> Vs. 1/[S]), and the results suggested a noncompetitive enzyme inhibition (K<sub>i</sub> = 0.17 μM) (Fig. 2).

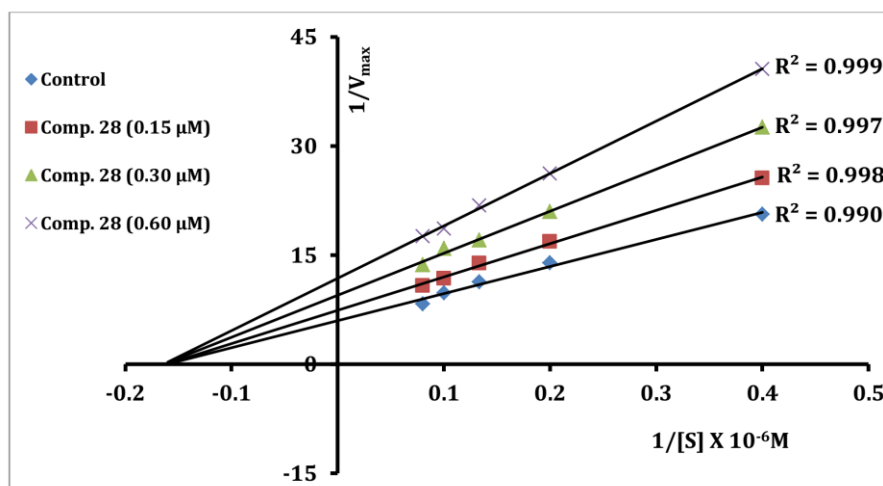


**Fig. 2.** Enzyme kinetics study of the inhibition of hAChE by compound **28**.

### 2.2.3 DPPH ( $\alpha, \alpha$ -diphenyl- $\beta$ -picrylhydrazyl) assay

The DPPH assay was used to determine the antioxidant activities of the synthesized compounds (**21-35**). Compounds **25**, **26**, **27** and **28**, containing hydrogen bond donating groups ( $-\text{NH}$  and  $-\text{OH}$ ), showed potential antioxidant activities (57.7, 63.4, 58.8 and 60.0%, respectively) by scavenging the DPPH free radical at a concentration of 20  $\mu\text{M}$ . The results of the DPPH assay are shown in Table 1.

### 2.2.4. Propidium iodide (PI) displacement assay

Compounds **25**, **26** and **28** were evaluated for PI displacement from the PAS-hAChE enzyme complex. The results revealed that compounds **25** (17.3%) and **28** (17.6%) considerably displaced PI from the PAS-hAChE complex. These results are comparable with those of donepezil (18.0%) (Table 2).

### 2.2.5 Blood-Brain Barrier (BBB) Permeation Assay

The parallel artificial membrane permeation assay (PAMPA-BBB) was performed to assess BBB permeability of compounds **25**, **26** and **28**, and the model was validated using nine commercial drugs. The results of the PAMPA-BBB assay indicated that compound **28** had higher permeability than compounds **25** and **26** through the BBB. Based on these results, compound **28** was selected for further biological evaluations (Table 2).

**Table 2.** The results of PI displacement and PAMPA-BBB assays.

Comp. Code	PI Displacement (%) <sup>a</sup>	PAMPA-BBB permeability $P_{e(exp)}$ ( $10^{-6}$ cm/s)	PAMPA-BBB Prediction (CNS+ <sup>b</sup> , CNS- <sup>c</sup> , CNS± <sup>d</sup> )
25	17.3 ± 0.9	4.21 ± 0.37	CNS±
26	13.6 ± 0.8	3.23 ± 0.23	CNS±
28	17.6 ± 1.3	5.82 ± 0.56	CNS+
donepezil	18.0 ± 1.2	6.89 ± 0.61	CNS+

<sup>a</sup>PI displacement assay was performed on hAChE, and the values are presented as the mean ± S.D. (n=3);

<sup>b</sup>‘CNS+’ (prediction of high BBB permeation);  $P_e$  ( $10^{-6}$  cm/s) > 4.3926; <sup>c</sup>‘CNS-’ (prediction of low BBB permeation);  $P_e$  ( $10^{-6}$  cm/s) < 1.7766; <sup>d</sup>‘CNS±’ (uncertain BBB permeation);  $P_e$  ( $10^{-6}$  cm/s) 4.3926 to 1.7766.

### 2.2.6 hAChE-induced A $\beta$ aggregation assay

According to the results of the PI displacement assay, compound **28** significantly interacts with PAS-hAChE. Therefore, its ability to inhibit hAChE-induced A $\beta$  aggregation was evaluated using the thioflavin T (ThT) assay. The outcome of the study revealed that its ability to inhibit hAChE-induced A $\beta$  aggregation was concentration dependent, and the highest inhibition was observed at a concentration ratio of 1:2 (A $\beta$ :inhibitor) (Fig. 3).

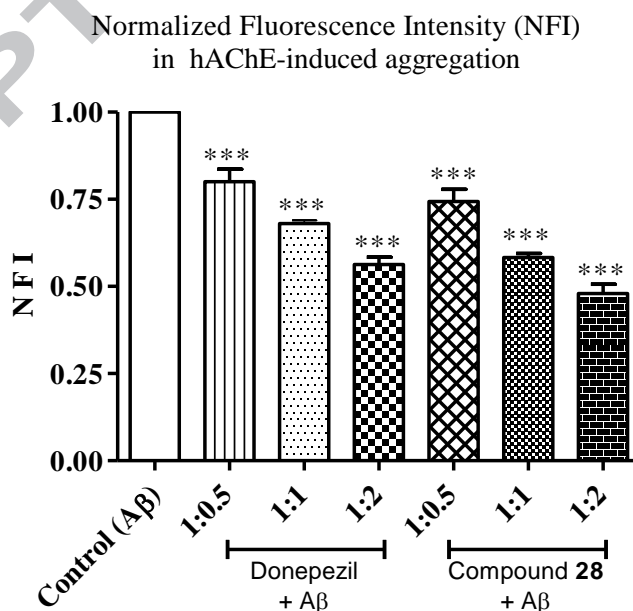


**Fig. 3.** Effects of donepezil and compound **28** on hAChE-induced A $\beta$  aggregation. \*\*\*  $p < 0.001$  compared to control. All values are expressed as the mean ± S.D. (n=3) of the normalized fluorescence intensity (NFI).

### 2.2.7 Neurotoxicity assay

Neuroblastoma SH-SY5Y cells are mostly used for assessing neurotoxicity owing to their high resemblance to mature human neurons.<sup>53</sup> The neurotoxicity of compound **28** was evaluated by an MTT-based colorimetric assay. The assay showed that compound **28** was not neurotoxic (Table 3).

**Table 3.** The results of neurotoxicity on the SH-SY5Y cell line.

Compound	IC <sub>50</sub> (μM) <sup>a</sup>
<b>28</b>	79.4 ± 5.9
donepezil	84.1 ± 6.9

<sup>a</sup>Values are expressed as the mean ± S.D. (n = 3).

### 2.2.8 Acute oral toxicity study

The acute toxicity of compound **28** was determined on healthy Swiss albino mice (25-30 g) following the OECD 423 guidelines. Several behavioral changes, cholinergic effects and toxic reactions, such as tremors, convulsions, salivation, diarrhea, sleep, lacrimation and feeding behavior, were monitored. There were no signs of any cholinergic side effects, and no toxicity or mortality was observed following the administration of test compound **28**. The study revealed that compound **28** has a significant safety margin.<sup>54</sup>

### 2.2.9 In vivo behavioral studies

Scopolamine-induced amnesia in mice is the standard model in behavioral pharmacology for the evaluation of AChE inhibitory potential. Scopolamine is a muscarinic antagonist, and its administration induces cognitive impairment through cholinergic deficit.<sup>55</sup>

#### 2.2.9.1 Y-maze test in mice

Compound **28** was assessed for its ability to enhance learning and memory against a scopolamine-induced cognitive deficit. The results showed a significantly decreased (<sup>\*\*\*</sup>p < 0.001) spontaneous alternation rate in scopolamine compared to the control. Treatment with compound **28** elicited a dose-dependent increase (2.5 mg/kg: <sup>##</sup>p < 0.01; 5 and 10 mg/kg: <sup>###</sup>p

< 0.001) in the spontaneous alternation rate compared to scopolamine (Fig. 4A). Additionally, the locomotive behavior of the scopolamine-treated mice did not change as confirmed by the nonsignificant changes in total arm entries among all groups (Fig. 4B).

#### 2.2.9.2 Passive avoidance test

The effect of treatment with compound **28** on scopolamine-induced memory impairment in mice was evaluated by a passive avoidance test. The transfer latency time (TLT) was calculated, and the respective groups in the acquisition and retention tests were compared. During the retention tests, the TLT of the scopolamine group was significantly lower than that of the control group, which signified an induction of memory impairment. There were nonsignificant differences between the TLT of the acquisition and retention tests in the scopolamine and vehicle groups. The TLT was significantly greater (\*\* $p < 0.001$ ) in mice treated with compound **28** compared to the corresponding acquisition test and the scopolamine group in the retention test. Moreover, treatment with compound **28** also prolonged TLT in a dose-dependent manner, which is similar to what was observed in the Y-maze experiment (Fig. 5).

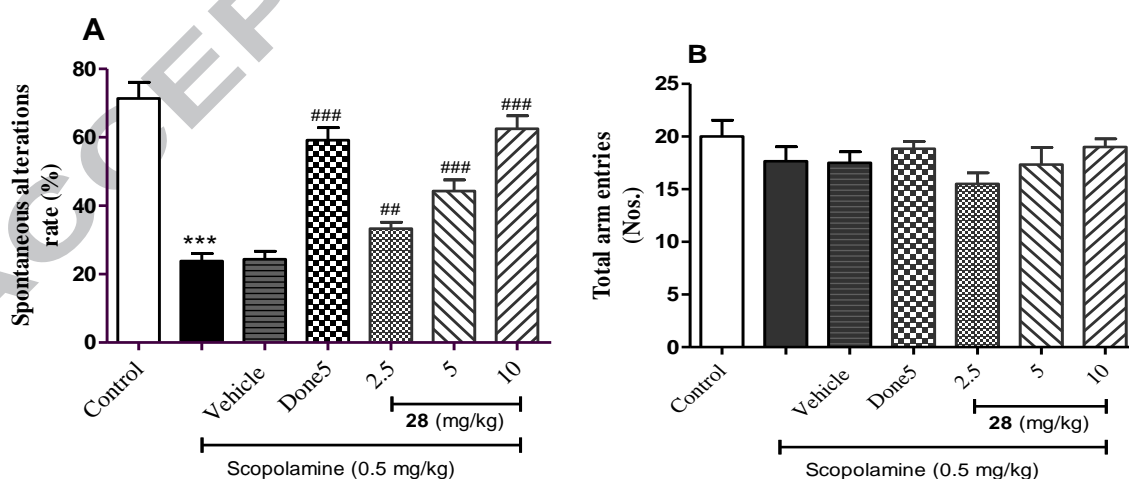


**Fig. 4.** Effect of treatment with compound **28** (2.5, 5 and 10 mg/kg, p.o.) on scopolamine-induced amnesia in a Y-maze test. (A) Spontaneous alternation rate; (B) total arm entries. Bars indicate the mean  $\pm$  S.D. ( $n = 6$ ); \*\*\*  $p < 0.001$  compared to the control; ###  $p < 0.001$ , ##  $p < 0.01$  compared to scopolamine; Done5 = donepezil.

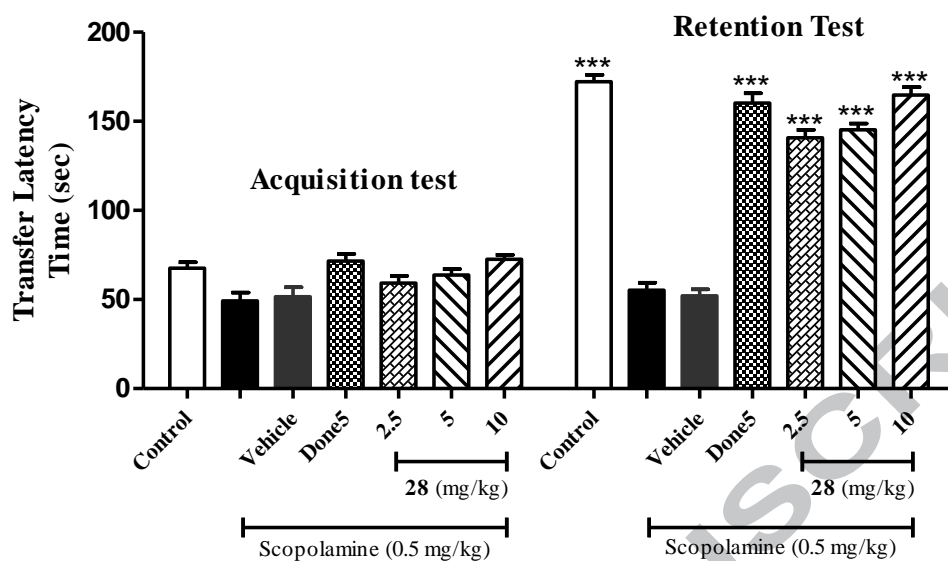


**Fig. 5.** Effect of treatment with compound **28** on scopolamine-induced memory impairment in a passive avoidance test. Bars indicate the mean  $\pm$  S.D. ( $n = 6$ ); \*\*\* $p < 0.001$  compared to the respective group in the acquisition test; Done5 = donepezil.

#### 2.2.10 *Ex vivo* estimation of AChE

The *ex vivo* estimation of AChE was performed using the Ellman assay with mouse brain homogenates. The results suggested that compound **28** (10 mg/kg) significantly reduced the rate of ACh hydrolysis via the inhibition of brain AChE. It also reflected that compound **28** was able to permeate the BBB (Fig. 6A), and the results were in agreement with those of the PAMPA-BBB assay.

#### 2.2.11 *Biochemical estimation of the oxidative stress factors*

Oxidative stress is a major detrimental factor associated with neurodegenerative disorders. Scopolamine is responsible for the induction of oxidative stress by altering the levels of several biochemical markers, such as malondialdehyde (MDA), total nonprotein thiol, and superoxide dismutase (SOD).<sup>21,56</sup> Therefore, compound **28** was investigated for its neuroprotective activity via the reduction of oxidative stress in cognitively impaired mice. The biochemical assessment of these biomarkers was performed using mouse brain homogenates.

### 2.2.11.1 2-Thiobarbituric acid-reactive substances (TBARS) assay

The TBARS method is widely used to estimate malondialdehyde (MDA) levels. The results revealed that scopolamine treatment caused a significant induction ( $^{***}p < 0.001$ ) in oxidative stress with increased levels of malondialdehyde (MDA) compared to the control. Compound **28** was not as active as scopolamine ( $^{###}p < 0.001$ ) in promoting oxidative stress (Fig. **6B**).

### 2.2.11.2 Assay of the total nonprotein thiol content

The method reported by Sedlak and Lindsay was used to determine the total nonprotein thiol contents in the brain samples.<sup>57,58</sup> The results indicated that scopolamine treatment significantly lowered ( $^{***}p < 0.001$ ) the total nonprotein thiol levels compared to the control group, suggesting an induction of oxidative stress. Compound **28** elevated the total nonprotein thiol levels ( $^{###}p < 0.001$ ) compared to the scopolamine-treated group (Fig. **6C**).

### 2.2.11.3 Superoxide dismutase (SOD) assay

Compound **28** showed a higher SOD level ( $^{###}p < 0.001$ ) compared to that of the scopolamine group, which reflects its ability to limit oxidative stress (Fig. **6D**). Overall, the results revealed that compound **28** (10 mg/kg) has significant antioxidant potential, and it can reverse scopolamine-induced oxidative stress to improve learning and memory.

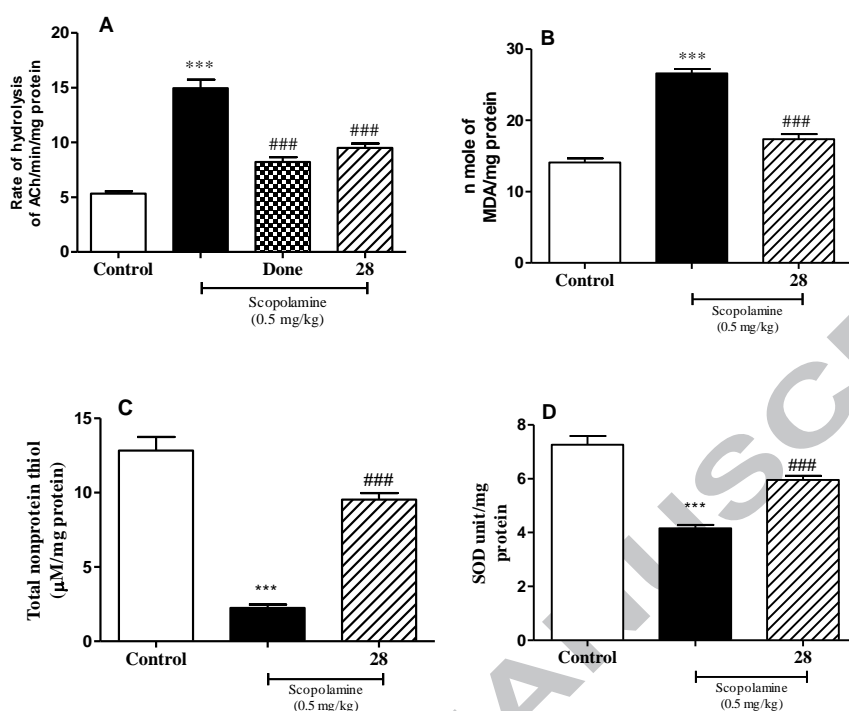


**Fig. 6.** The results of *ex vivo* and biochemical analysis. (A) AChE activity; (B) MDA level; (C) total nonprotein thiol content; (D) SOD level. The values are presented as the mean  $\pm$  S.D. ( $n = 6$ ); \*\*\*  $p < 0.001$  compared to the control; ###  $p < 0.001$  compared to scopolamine.

## 2.3. Computational Studies

### 2.3.1 *In silico* molecular docking studies

A molecular docking study was performed to assess the binding affinity and pose stability of compound **28** in the active sites of hAChE (PDB Code: 4EY7) using the Glide module of Schrödinger Maestro 2018-1. The cocrystallized Aricept (donepezil) ligand was extracted and redocked in the hAChE grid for validation of the docking parameters. The poses of the cocrystallized and redocked ligands were compared using a superposition tool, and the RMSD value was found to be 0.2 Å (Supp. Fig. S2).

Compound **28** and donepezil showed docked scores of -13.8 and -14.6 kcal/mole, respectively. The naphthyl group of compound **28** exhibited  $\pi$ - $\pi$  stacking and polar interactions with His447 in the catalytic active site (CAS). Additionally, compound **28** formed a polar interaction with Ser203 in the CAS. Compound **28** interacted with all PAS

residues through hydrophobic interactions (Tyr72, Tyr124, Trp286 and Tyr341) and electrostatic interactions (Asp74). At the anionic subsite, compound **28** formed hydrophobic interactions with Trp86 and Phe338 and electrostatic interactions with the Glu202 residue. The N-atom of 4-AP interacted with the Phe295 residue in the acyl binding pocket through H-bonding interactions. At the oxyanion site, compound **28** interacted with Gly121 and Gly122 and formed hydrophobic interactions with Ala204 (Fig. 7A, 7B and Table 4).

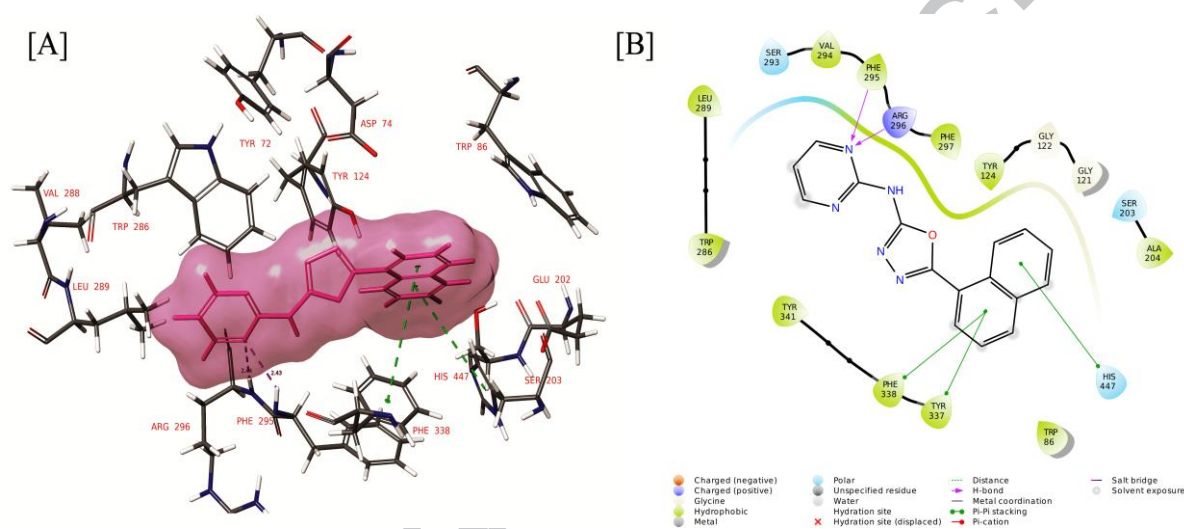


**Fig. 7.** The docking of compound **28** in the hAChE enzyme. (A) Image of the 3D interactions of compound **28** in the ligand binding surface (pink color) with the active site residues of hAChE; (B) 2D image showing the active site interactions.

**Table 4.** Detailed analysis of the molecular docking interaction of compound **28** and donepezil in hAChE (4EY7).

Comp.	CAS	PAS	Interacting residues <sup>#</sup>		
			Anionic subsite	Acyl binding pocket	Other interacting residues
<b>28</b>	Ser203 <sup>a</sup> , His447 <sup>a,b</sup>	Tyr72 <sup>c</sup> , Asp74 <sup>d</sup> , Tyr124 <sup>c</sup> , Trp286 <sup>c</sup> , Tyr341 <sup>c</sup>	Trp86 <sup>c</sup> , Phe338 <sup>b,c</sup> , Glu202 <sup>d</sup>	Phe295 <sup>c,e</sup> , Phe297 <sup>c</sup>	Ala204 <sup>c</sup> , Val294 <sup>c</sup> , Gly441 <sup>c</sup> , Leu289 <sup>c</sup> , Ser293 <sup>a</sup> , Tyr337 <sup>c</sup> , Arg296 <sup>d</sup> , Gly121 <sup>c,f</sup> , Gly122 <sup>c</sup>
donepezil	Ser203 <sup>a</sup> , His447 <sup>a</sup>	Tyr72 <sup>c</sup> , Tyr124 <sup>c</sup> , Trp286 <sup>b,c</sup> , Tyr341 <sup>c</sup>	Trp86 <sup>b,c,g</sup> , Phe338 <sup>b,c,g</sup>	Phe295 <sup>c,e</sup> , Phe297 <sup>c</sup>	Gly120 <sup>c,f</sup> , Gly121 <sup>c,f</sup> , Tyr133 <sup>c</sup> , Leu289 <sup>c</sup> , Val294 <sup>c</sup> , Tyr337 <sup>c</sup> , Gly448 <sup>c</sup> , Ile451 <sup>c</sup>

<sup>#</sup> All the interacting residues are within the 4 Å distance with the ligand; <sup>a</sup> polar; <sup>b</sup>  $\pi$ - $\pi$  stacking; <sup>c</sup> hydrophobic; <sup>d</sup> electrostatic; <sup>e</sup> H-bonding; <sup>f</sup> glycine and <sup>g</sup>  $\pi$ -cation interactions.

### 2.3.2 Molecular dynamics (MD) simulations

A 30 nsec MD simulation was performed to affirm the binding pose stability of the compound **28**-hAChE docked complex. The generated trajectories were utilized to produce simulation interaction diagrams, and the results were analyzed. The stability of the docked protein-ligand complex was determined by RMSD (root mean square deviation) and RMSF (root mean square fluctuation) calculations. The protein-ligand RMSD showed initial fluctuations up to 6.25 nsec before stabilizing. The docked complex was compared to the reference protein backbone structure, which was stabilized and found to be within 1-3 Å (Fig. 8). The structural stability of the protein and compound **28** was also evaluated based on the RMSF value, which was found to be less than 3 Å and confirmed the absence of overall local changes along the protein chain and positions of the atoms in the ligand (Supp. Fig. S3).

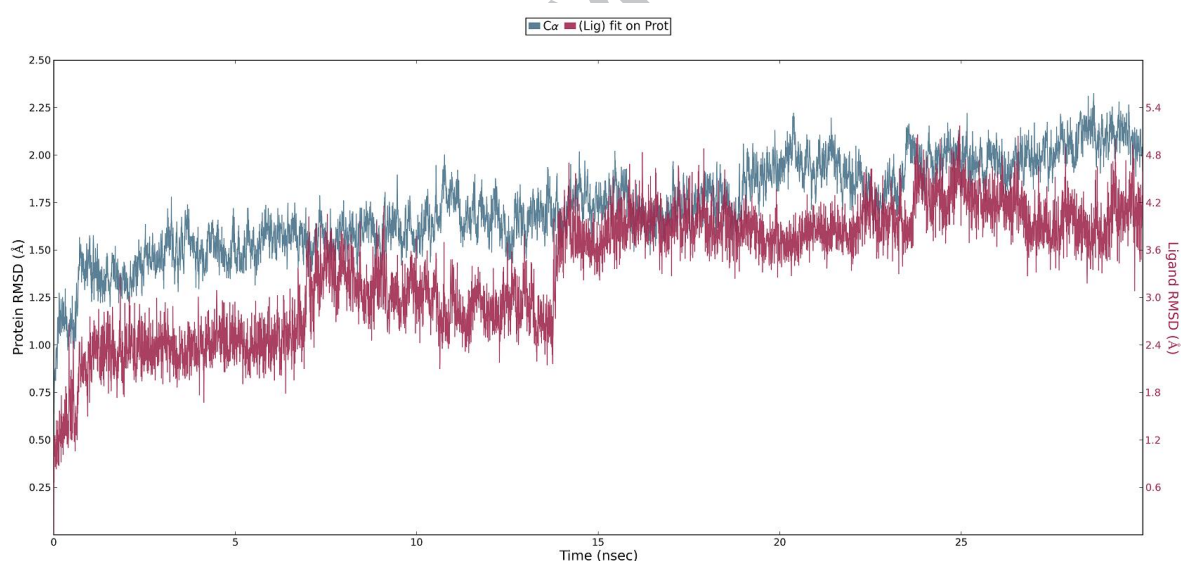


**Fig. 8.** RMSD graph of the docked compound **28**-hAChE complex from 30 nsec MD simulations.

The results of the MD simulations were analyzed using simulation interaction diagrams. The representation of the interaction analysis through stacked bar charts (Fig. 9A) showed the normalized value of the interaction fractions over the course of the trajectory. For example, the value of 0.6 suggests that a specific interaction was maintained for 60% of the simulation period. The results suggested that the interaction between compound **28** and the PAS residues

remained intact throughout the simulation. The detailed analysis showed that compound **28** interacted through H bonding, hydrophobic interactions and salt-bridge formation with Tyr72, Asp74, Tyr124, Trp286 and Tyr341 in the PAS with interaction fractions of 0.52, 0.68, 0.69, 0.74 and 0.81, respectively.

Furthermore, interaction analysis was represented graphically (**Fig. 9B**) to show the H-bonding and hydrophobic interactions that existed for more than 20% of the total simulation run time. The results showed that the nitrogen atom of 2-AP exhibited H-bonding interactions with Asp74 (20%) and Trp286 (22%) at the PAS. Additionally, Asp74 showed H-bonding interactions (21%) with the –NH linker. Furthermore, the results suggested a hydrophobic interaction between compound **28** and the Tyr341 residue at the PAS.

The results of the MD simulation analysis were also analyzed as a function of time (**Fig. 9C**). The top panel of a timeline representation shows the total number of specific contacts (H-bonding, hydrophobic, ionic, and water bridge interactions) between the protein and the ligand over the course of the simulation run. The bottom panel shows the interactions of individual amino acid residues in each trajectory frame during the simulation run. Some residues formed more than one specific interaction with the ligand, which was represented by a darker shade of orange according to the scale at the right of the plot. Overall, the results of the MD simulation analysis suggested stable and effective interactions between compound **28** and the PAS, and the results were found to be in agreement with those of the PI displacement assay.

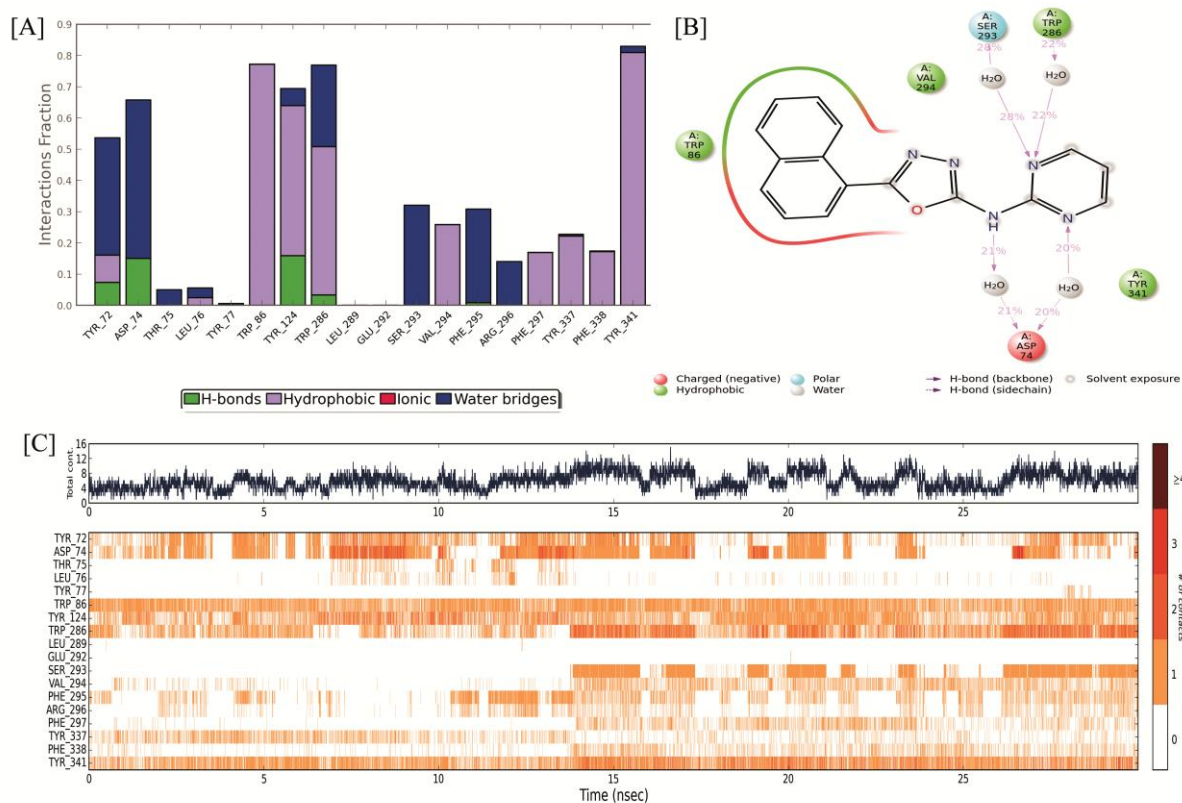


**Fig. 9.** MD simulation analysis of the compound **28**-hAChE docked complex. (A) Stacked bar chart showing interaction fractions; (B) graphical representation showing percentage interactions with active site residues; (C) timeline representation.

### 3. CONCLUSION

Herein, we designed and synthesized a novel set of multitarget-directed molecules with both a 2-AP moiety and a substituted 1,3,4-oxadiazole ring for the treatment of cognitive dysfunctions. Among all the synthesized derivatives, naphthyl group-bearing compound **28** showed the highest *in vitro* hAChE inhibitory activity ( $pIC_{50} = 6.52$ ) with a noncompetitive enzyme inhibition ( $K_i = 0.17 \mu M$ ). Among the evaluated derivatives, the antioxidant activity of compound **28** (60.0%) was found to be comparable with that of ascorbic acid (64.6%), which was used as a standard. Furthermore, compound **28** significantly displaced propidium iodide (17.6%) from the PAS-hAChE complex in the PI assay and showed significant BBB penetrability. Compound **28** also inhibited hAChE-induced A $\beta$  aggregation in a concentration-dependent manner based on the thioflavin T assay. Additionally, the MTT assay with the SH-SY5Y neuroblastoma cell line suggested that compound **28** is devoid of

neurotoxicity. *In vivo* behavioral studies revealed that compound **28** (10 mg/kg) significantly reversed the scopolamine-induced cognitive dysfunctions in mice as evaluated by Y-maze and passive avoidance tests. The *ex vivo* and biochemical analysis of compound **28** showed significant brain AChE inhibition and antioxidant activities, respectively. The computational studies corroborated the pharmacological outcomes owing to the effective interactions between compound **28** and the active site residues of PAS. Thus, this study indicated that multitargeted *N*-(pyrimidin-2-yl)-1,3,4-oxadiazole derivatives are potential scaffolds for the treatment of dementia with compound **28** as a promising lead for further research.

## 4. EXPERIMENTAL

### 4.1. Chemistry

#### 4.1.1 Chemicals and Instrumentation

Chemicals and solvents were purchased from Sigma-Aldrich, TCI chemicals and Avra Synthesis Pvt Ltd., India and were used without further purification. The progress of each reaction was monitored by TLC. Melting points were determined using open capillary tubes on a Stuart melting point apparatus (SMP10) and are uncorrected. FT-IR spectra were recorded on an Alpha ECO-ATR Spectrophotometer (Bruker, USA). <sup>1</sup>H NMR (500 MHz) and <sup>13</sup>C NMR (125 MHz) spectra were recorded (Bruker Avance FT-NMR spectrophotometer, USA) in deuterated solvent (DMSO-*d*<sub>6</sub>) using tetramethylsilane (TMS) as an internal standard; the chemical shifts ( $\delta$ , ppm) and coupling constants (*J*, Hz) are reported. Elemental analyses (C, H, N) were performed on an EXETER CE-440 elemental analyzer.

#### 4.1.2 Synthesis of phenyl pyrimidin-2-ylcarbamate (2)

2-AP (**1**; 31.54 mmol) was dissolved in dry DCM in the presence of pyridine (44.16 mmol). Following the addition of PCF (37.85 mmol) under a nitrogen blanket, the reaction mixture was stirred for 3 h at 0-5 °C. After completion of the reaction (monitored by TLC), the reaction mixture was concentrated *in vacuo* to obtain a solid. This solid was suspended in 60

ml of petroleum ether and 50 ml of distilled water. The resulting suspension was filtered and washed with water (500 ml) and petroleum ether (100 ml) to yield pure compound **2** as a yellow solid.

Yield: 79%; mp 201-203 °C; FT-IR (ATR,  $\nu$   $\text{cm}^{-1}$ ): 3203 (-NH), 1720 (>C=O);  $^1\text{H}$  NMR (500 MHz,  $\delta_{\text{H}}$ , DMSO- $d_6$ ): 11.31 (s, 1H), 8.59 (d, 2H,  $J = 5.0$ ), 7.45 (d, 2H,  $J = 7.5$ ), 7.33-7.24 (m, 3H), 7.15 (t, 1H,  $J = 4.5$  Hz);  $^{13}\text{C}$  NMR (125 MHz,  $\delta_{\text{C}}$ , DMSO- $d_6$ ): 158.7, 158.3, 156.3, 151.2, 149.2, 128.8, 124.5, 122.1, 114.6. Anal.  $\text{C}_{11}\text{H}_9\text{N}_3\text{O}_2$ : C, 61.39; H, 4.22; N, 19.53; Found: C, 61.46; H, 4.18; N, 19.50.

#### 4.1.3. Synthesis of *N*-(pyrimidin-2-yl)hydrazinecarboxamide (**3**)

Compound (**2**; 2.32 mmol) and 85% v/v hydrazine hydrate (10.45 mmol) were dissolved in absolute ethanol and heated at 70 °C for 30 min. The reaction mixture was cooled and filtered, and the solid was washed with absolute ethanol and dried to afford **3** as an off-white solid.

Yield: 81%. mp 235-237 °C; FT-IR (ATR,  $\nu$   $\text{cm}^{-1}$ ): 3260, 3240 (-NH<sub>2</sub>), 3201 (NHCONH), 1698 (>C=O);  $^1\text{H}$  NMR (500 MHz,  $\delta_{\text{H}}$ , DMSO- $d_6$ ): 9.87 (s, 1H), 9.65 (s, 1H), 8.58 (d, 2H,  $J = 5.0$ ), 7.05 (t, 1H,  $J = 4.5$  Hz), 4.24 (s, 2H).  $^{13}\text{C}$  NMR (125 MHz,  $\delta_{\text{C}}$ , DMSO- $d_6$ ): 158.5, 158.4, 156.3, 114.9. Anal.  $\text{C}_5\text{H}_7\text{N}_5\text{O}$ : C, 39.21; H, 4.61; N, 45.73; Found: C, 39.16; H, 4.64; N, 45.70.

#### 4.1.4 General procedure for the synthesis of compounds 4-18

Compound **3** (4.24 mmol) and the appropriate aromatic aldehyde (8.24 mmol) were dissolved in absolute ethanol (30 ml) and refluxed for 3 h. The reaction mixture was allowed to cool to room temperature and then filtered. The resulting solid was washed with absolute ethanol and dried in a rotary vacuum evaporator to yield the title compounds (**4-18**).

**(E)-2-benzylidene-N-(pyrimidin-2-yl)hydrazine-1-carboxamide (4)**

Yield: 63%. mp: 207-209 °C; FT-IR (ATR,  $\nu$  cm<sup>-1</sup>): 3340, 3231 (NHCONH), 1701 (>C=O), 1578 (-C=N); <sup>1</sup>H NMR (500 MHz,  $\delta$ <sub>H</sub>, DMSO-*d*<sub>6</sub>): 12.40 (brs, 1H), 10.15 (brs, 1H), 8.64 (d, 2H, *J* = 4.5 Hz), 8.27 (s, 1H), 7.72 (d, 2H, *J* = 7.0 Hz) 7.45- 7.40 (m, 3H), 7.13 (t, 1H, *J* = 7.0 Hz); <sup>13</sup>C NMR (125 MHz,  $\delta$ <sub>C</sub>, DMSO-*d*<sub>6</sub>): 158.7, 158.0, 151.4, 134.7, 130.2, 129.2, 127.3, 115.8. Anal. C<sub>12</sub>H<sub>11</sub>N<sub>5</sub>O: C, 59.74; H, 4.60; N, 29.03; Found: C, 59.69; H, 4.63; N, 29.00.

**(E)-2-(4-methylbenzylidene)-N-(pyrimidin-2-yl)hydrazine-1-carboxamide (5)**

Yield: 61%; mp: 200-202 °C; FT-IR (ATR,  $\nu$  cm<sup>-1</sup>): 3311, 3223 (NHCONH), 1693 (>C=O), 1567 (-C=N); <sup>1</sup>H NMR (500 MHz,  $\delta$ <sub>H</sub>, DMSO-*d*<sub>6</sub>): 12.33 (brs, 1H), 10.13 (brs, 1H), 8.64 (d, 2H, *J* = 4.5 Hz), 8.24 (brs, 1H), 7.61 (d, 2H, *J* = 7.5 Hz) 7.26 (d, 2H, *J* = 8.0 Hz), 7.13 (t, 1H, *J* = 7.0 Hz), 2.34 (s, 3H); <sup>13</sup>C NMR (125 MHz,  $\delta$ <sub>C</sub>, DMSO-*d*<sub>6</sub>): 157.5, 156.1, 139.3, 139.1, 132.5, 132.3, 129.6, 127.2, 127.1, 114.9, 21.4; Anal. C<sub>13</sub>H<sub>13</sub>N<sub>5</sub>O: C, 61.17; H, 5.13; N, 27.43; Found: C, 61.25; H, 5.10; N, 27.45.

**(E)-2-(4-methoxybenzylidene)-N-(pyrimidin-2-yl)hydrazine-1-carboxamide (6)**

Yield: 78%; mp: 188-190 °C; FT-IR (ATR,  $\nu$  cm<sup>-1</sup>): 3323, 3214 (NHCONH), 1709 (>C=O), 1574 (-C=N); <sup>1</sup>H NMR (500 MHz,  $\delta$ <sub>H</sub>, DMSO-*d*<sub>6</sub>): 12.31 (brs, 1H), 10.11 (brs, 1H), 8.63 (d, 2H, *J* = 4.5 Hz), 8.21 (brs, 1H), 7.66 (d, 2H, *J* = 8.5 Hz) 7.12 (s, 1H), 7.00- 6.83 (m, 2H), 3.73 (s, 3H); <sup>13</sup>C NMR (125 MHz,  $\delta$ <sub>C</sub>, DMSO-*d*<sub>6</sub>): 161.0, 158.7, 158.5, 158.0, 151.4, 130.4, 128.9, 127.3, 115.5, 114.6, 110.6, 55.7; Anal. C<sub>13</sub>H<sub>13</sub>N<sub>5</sub>O<sub>2</sub>: C, 57.56; H, 4.83; N, 25.82; Found: C, 57.50; H, 4.81; N, 25.85.

**(E)-2-(3,4-dimethoxybenzylidene)-N-(pyrimidin-2-yl)hydrazine-1-carboxamide (7)**

Yield: 84%; mp: 216-218 °C; FT-IR (ATR,  $\nu$  cm<sup>-1</sup>): 3298, 3212 (NHCONH), 1691 (>C=O), 1580 (-C=N); <sup>1</sup>H NMR (500 MHz,  $\delta$ <sub>H</sub>, DMSO-*d*<sub>6</sub>): 12.31 (brs, 1H), 10.10 (brs, 1H), 8.65 (d, 2H, *J* = 4.5 Hz), 8.22 (brs, 1H), 7.34 (s, 1H) 7.21 (q, 1H, *J* = 1.5 Hz), 7.14 (t, 1H, *J* = 5.0 Hz), 7.03 (d, 1H, *J* = 8.5 Hz), 3.82 (s, 6H); <sup>13</sup>C NMR (125 MHz,  $\delta$ <sub>C</sub>, DMSO-*d*<sub>6</sub>): 158.7, 158.1,

151.3, 150.9, 149.5, 121.7, 112.0, 56.0; Anal. C<sub>14</sub>H<sub>15</sub>N<sub>5</sub>O<sub>3</sub>: C, 55.81; H, 5.02; N, 23.24; Found: C, 55.89; H, 4.99; N, 23.26.

***(E)-2-(3,4,5-trimethoxybenzylidene)-N-(pyrimidin-2-yl)hydrazine-1-carboxamide (8)***

Yield: 74%; mp: 190-192 °C; FT-IR (ATR,  $\nu$  cm<sup>-1</sup>): 3312, 3239 (NHCONH), 1699 (>C=O), 1584 (-C=N); <sup>1</sup>H NMR (500 MHz,  $\delta_{\text{H}}$ , DMSO-*d*<sub>6</sub>): 12.42 (brs, 1H), 10.18 (brs, 1H), 8.63 (brs, 2H), 8.21 (brs, 1H), 7.20-7.04 (m, 3H), 3.82 (s, 6H), 3.69 (s, 3H); <sup>13</sup>C NMR (125 MHz,  $\delta_{\text{C}}$ , DMSO-*d*<sub>6</sub>): 158.7, 158.0, 153.5, 151.5, 139.3, 130.2, 115.7, 104.6, 60.5, 56.3; Anal. C<sub>15</sub>H<sub>17</sub>N<sub>5</sub>O<sub>4</sub>: C, 54.38; H, 5.17; N, 21.14; Found: C, 54.46; H, 5.20; N, 21.11.

***(E)-2-(4-hydroxybenzylidene)-N-(pyrimidin-2-yl)hydrazine-1-carboxamide (9)***

Yield: 71%; mp: 225-227 °C; FT-IR (ATR,  $\nu$  cm<sup>-1</sup>): 3420 (-OH), 3322, 3231 (NHCONH), 1697 (>C=O), 1579 (-C=N); <sup>1</sup>H NMR (500 MHz,  $\delta_{\text{H}}$ , DMSO-*d*<sub>6</sub>): 12.23 (brs, 1H), 10.12 (brs, 1H), 9.88 (s, 1H), 8.64 (d, 2H, *J* = 5.0 Hz), 8.21 (brs, 1H), 7.55 (d, 2H), 7.13 (s, 1H), 6.83 (d, 2H); <sup>13</sup>C NMR (125 MHz,  $\delta_{\text{C}}$ , DMSO-*d*<sub>6</sub>): 159.6, 158.7, 158.1, 151.2, 129.0, 125.8, 116.1, 114.8; Anal. C<sub>12</sub>H<sub>11</sub>N<sub>5</sub>O<sub>2</sub>: C, 56.03; H, 4.31; N, 27.22; Found: C, 56.11; H, 4.27; N, 27.19.

***(E)-2-(2-hydroxybenzylidene)-N-(pyrimidin-2-yl)hydrazine-1-carboxamide (10)***

Yield: 79%; mp: 215-217 °C; FT-IR (ATR,  $\nu$  cm<sup>-1</sup>): 3412 (-OH), 3301, 3243 (NHCONH), 1701 (>C=O), 1572 (-C=N); <sup>1</sup>H NMR (500 MHz,  $\delta_{\text{H}}$ , DMSO-*d*<sub>6</sub>): 12.43 (brs, 1H), 11.14 (brs, 1H), 10.29 (brs, 1H), 8.66 (d, 2H, *J* = 5.0 Hz), 8.54 (s, 1H), 7.29-7.26 (m, 2H), 7.15 (t, 1H, *J* = 5.3 Hz), 6.91 (t, 2H, *J* = 7.8 Hz); <sup>13</sup>C NMR (125 MHz,  $\delta_{\text{C}}$ , DMSO-*d*<sub>6</sub>): 158.7, 158.0, 157.2, 151.2, 131.4, 129.1, 119.7, 116.7, 115.7; Anal. C<sub>12</sub>H<sub>11</sub>N<sub>5</sub>O<sub>2</sub>: C, 56.03; H, 4.31; N, 27.22; Found: C, 55.94; H, 4.26; N, 27.17.

***(E)-2-(naphthalen-1-ylmethylene)-N-(pyrimidin-2-yl)hydrazine-1-carboxamide (11)***

Yield: 69%; mp: 218-220 °C; FT-IR (ATR,  $\nu$  cm<sup>-1</sup>): 3310, 3234 (NHCONH), 1699 (>C=O), 1579 (-C=N); <sup>1</sup>H NMR (500 MHz,  $\delta_{\text{H}}$ , DMSO-*d*<sub>6</sub>): 12.55 (brs, 1H), 10.21 (brs, 1H), 8.97 (d, 2H, *J* = 5.0 Hz), 8.68 (d, 2H, *J* = 5.0 Hz), 8.00 (d, 3H, *J* = 4.8 Hz), 7.67-7.60 (m, 3H), 7.16 (t,

1H,  $J = 4.5$  Hz);  $^{13}\text{C}$  NMR (125 MHz,  $\delta_{\text{C}}$ , DMSO- $d_6$ ): 158.7, 158.5, 158.0, 151.5, 133.9, 130.6, 130.1, 129.1, 127.6, 126.7, 124.7, 124.5, 115.7, 110.7; Anal.  $\text{C}_{16}\text{H}_{13}\text{N}_5\text{O}$ : C, 65.97; H, 4.50; N, 24.04; Found: C, 65.91; H, 4.47; N, 24.01.

***(E)-2-(4-fluorobenzylidene)-N-(pyrimidin-2-yl)hydrazine-1-carboxamide (12)***

Yield: 65%; mp: 205-207 °C; FT-IR (ATR,  $\nu$   $\text{cm}^{-1}$ ): 3310, 3236 (NHCONH), 1705 ( $>\text{C}=\text{O}$ ), 1583 ( $-\text{C}=\text{N}$ );  $^1\text{H}$  NMR (500 MHz,  $\delta_{\text{H}}$ , DMSO- $d_6$ ): 12.40 (brs, 1H), 10.17 (brs, 1H), 8.67-8.63 (m, 2H), 8.27 (s, 1H), 7.79-7.76 (m, 2H), 7.25 (t, 2H,  $J = 4.5$  Hz), 7.13 (t, 1H,  $J = 4.0$ );  $^{13}\text{C}$  NMR (125 MHz,  $\delta_{\text{C}}$ , DMSO- $d_6$ ): 164.3, 162.4, 158.7, 158.5, 158.9, 151.5, 131.2, 129.5, 116.1, 110.7; Anal.  $\text{C}_{12}\text{H}_{10}\text{FN}_5\text{O}$ : C, 55.60; H, 3.89; N, 27.02; Found: C, 55.53; H, 3.92; N, 26.99.

***(E)-2-(4-chlorobenzylidene)-N-(pyrimidin-2-yl)hydrazine-1-carboxamide (13)***

Yield: 72%; mp: 220-222 °C; FT-IR (ATR,  $\nu$   $\text{cm}^{-1}$ ): 3311, 3232 (NHCONH), 1708 ( $>\text{C}=\text{O}$ ), 1579 ( $-\text{C}=\text{N}$ );  $^1\text{H}$  NMR (500 MHz,  $\delta_{\text{H}}$ , DMSO- $d_6$ ): 12.42 (brs, 1H), 10.18 (brs, 1H), 8.63 (d, 2H,  $J = 4.5$  Hz), 8.26 (s, 1H), 7.74 (d, 2H,  $J = 7.5$  Hz), 7.49 (d, 2H,  $J = 8.0$  Hz), 7.13 (s, 1H);  $^{13}\text{C}$  NMR (125 MHz,  $\delta_{\text{C}}$ , DMSO- $d_6$ ): 158.7, 157.9, 151.5, 134.6, 133.6, 130.5, 129.3, 129.0, 115.8; Anal.  $\text{C}_{12}\text{H}_{10}\text{ClN}_5\text{O}$ : C, 52.28; H, 3.66; N, 25.40; Found: C, 52.32; H, 3.63; N, 25.37.

***(E)-2-(4-bromobenzylidene)-N-(pyrimidin-2-yl)hydrazine-1-carboxamide (14)***

Yield: 71%; mp: 215-217 °C; FT-IR (ATR,  $\nu$   $\text{cm}^{-1}$ ): 3301, 3239 (NHCONH), 1690 ( $>\text{C}=\text{O}$ ), 1584 ( $-\text{C}=\text{N}$ );  $^1\text{H}$  NMR (500 MHz,  $\delta_{\text{H}}$ , DMSO- $d_6$ ): 12.43 (brs, 1H), 10.19 (brs, 1H), 8.63 (d, 2H,  $J = 4.5$  Hz), 8.21 (s, 1H), 8.25-8.20 (m, 4H), 7.14 (t, 1H,  $J = 7.5$  Hz);  $^{13}\text{C}$  NMR (125 MHz,  $\delta_{\text{C}}$ , DMSO- $d_6$ ): 158.7, 157.9, 151.4, 134.0, 132.2, 129.2, 123.4, 114.1; Anal.  $\text{C}_{12}\text{H}_{10}\text{BrN}_5\text{O}$ : C, 45.02; H, 3.15; N, 21.88 Found: C, 44.96; H, 3.11; N, 21.92.

***(E)-2-(3-bromobenzylidene)-N-(pyrimidin-2-yl)hydrazine-1-carboxamide (15)***

Yield: 74%; mp: 210-212 °C; FT-IR (ATR,  $\nu$   $\text{cm}^{-1}$ ): 3311, 3201 (NHCONH), 1698 ( $>\text{C}=\text{O}$ ), 1569 ( $-\text{C}=\text{N}$ );  $^1\text{H}$  NMR (500 MHz,  $\delta_{\text{H}}$ , DMSO- $d_6$ ): 12.46 (brs, 1H), 10.19 (brs, 1H), 8.64 (d,

2H,  $J = 4.5$  Hz), 8.21 (s, 1H), 7.94 (s, 1H), 7.70-6.52 (m, 4H);  $^{13}\text{C}$  NMR (125 MHz,  $\delta_{\text{C}}$ , DMSO- $d_6$ ): 158.7, 158.0, 151.5, 132.7, 131.4, 129.3, 126.5, 122.5, 115.1; Anal.  $\text{C}_{12}\text{H}_{10}\text{BrN}_5\text{O}$ : C, 45.02; H, 3.15; N, 21.88 Found: C, 44.95; H, 3.17; N, 21.85.

**(E)-2-(2-chlorobenzylidene)-N-(pyrimidin-2-yl)hydrazine-1-carboxamide (16)**

Yield: 82%; mp: 200-202 °C; FT-IR (ATR,  $\nu$   $\text{cm}^{-1}$ ): 3302, 3239 (NHCONH), 1708 ( $>\text{C}=\text{O}$ ), 1576 ( $-\text{C}=\text{N}$ );  $^1\text{H}$  NMR (500 MHz,  $\delta_{\text{H}}$ , DMSO- $d_6$ ): 12.29 (brs, 1H), 10.02 (brs, 1H), 8.67 (d, 2H,  $J = 4.5$  Hz), 8.55 (s, 1H), 8.06 (s, 1H), 7.52-7.41 (m, 3H), 7.16 (t, 1H,  $J = 8.0$  Hz);  $^{13}\text{C}$  NMR (125 MHz,  $\delta_{\text{C}}$ , DMSO- $d_6$ ): 158.8, 158.0, 151.2, 133.2, 132.0, 131.5, 130.3, 127.9, 127.5, 116.1; Anal.  $\text{C}_{12}\text{H}_{10}\text{ClN}_5\text{O}$ : C, 52.28; H, 3.66; N, 25.40; Found: C, 52.36; H, 3.69; N, 25.37.

**(E)-2-(4-nitrobenzylidene)-N-(pyrimidin-2-yl)hydrazine-1-carboxamide (17)**

Yield: 77%; mp: 279-281 °C; FT-IR (ATR,  $\nu$   $\text{cm}^{-1}$ ): 3312, 3231 (NHCONH), 1713 ( $>\text{C}=\text{O}$ ), 1581 ( $-\text{C}=\text{N}$ );  $^1\text{H}$  NMR (500 MHz,  $\delta_{\text{H}}$ , DMSO- $d_6$ ): 12.42 (brs, 1H), 10.11 (brs, 1H), 8.67 (m, 1H), 8.38-8.29 (m, 4H), 8.16 (d, 1H), 7.99 (d, 1H), 7.16 (d, 1H,  $J = 8.0$  Hz);  $^{13}\text{C}$  NMR (125 MHz,  $\delta_{\text{C}}$ , DMSO- $d_6$ ): 158.7, 158.0, 151.3, 148.0, 130.0, 128.2, 124.6, 124.5, 114.1; Anal.  $\text{C}_{12}\text{H}_{10}\text{N}_6\text{O}_3$ : C, 50.35; H, 3.52; N, 29.36; Found: C, 50.27; H, 3.55; N, 29.34.

**(E)-2-(2-nitrobenzylidene)-N-(pyrimidin-2-yl)hydrazine-1-carboxamide (18)**

Yield: 70%; mp: 235-237 °C; FT-IR (ATR,  $\nu$   $\text{cm}^{-1}$ ): 3315, 3227 (NHCONH), 1702 ( $>\text{C}=\text{O}$ ), 1578 ( $-\text{C}=\text{N}$ );  $^1\text{H}$  NMR (500 MHz,  $\delta_{\text{H}}$ , DMSO- $d_6$ ): 12.39 (brs, 1H), 10.09 (brs, 1H), 8.65 (d, 2H), 8.55 (s, 1H), 8.21-8.14 (m, 2H), 8.05 -7.64 (m, 3H);  $^{13}\text{C}$  NMR (125 MHz,  $\delta_{\text{C}}$ , DMSO- $d_6$ ): 158.8, 158.5, 157.9, 151.4, 148.4, 134.1, 130.9, 128.9, 126.9, 124.6, 110.7; Anal.  $\text{C}_{12}\text{H}_{10}\text{N}_6\text{O}_3$ : C, 50.35; H, 3.52; N, 29.36; Found: C, 50.31; H, 3.49; N, 29.35.

**4.1.5 General procedure for the synthesis of compounds 19-20**

Compounds **7** and **18** (1.87 mmol) were used for the synthesis of compounds **19** and **20**, respectively. Compound **7** or **18** was dissolved in dry methanol, sodium borohydride

(NaBH<sub>4</sub>) was added, and the reaction mixture was stirred for 1 h at 0-5 °C. The solvent was evaporated *in vacuo* to yield a crude product that was recrystallized from absolute ethanol to afford the desired compound (**19** or **20**).

**2-(3,4-dimethoxybenzyl)-N-(pyrimidin-2-yl)hydrazine-1-carboxamide (19)**

Yield: 65%; mp 211-213 °C; FT-IR (ATR,  $\nu$  cm<sup>-1</sup>): 3379 (-NH), 3215 (NHCONH), 1699 (>C=O); <sup>1</sup>H NMR (500 MHz,  $\delta$ <sub>H</sub>, DMSO-*d*<sub>6</sub>): 12.35 (brs, 1H), 10.12 (brs, 1H), 8.61-8.19 (m, 2H), 7.31-7.23 (m, 2H), 7.17-7.09 (m, 2H), 3.82 (s, 6H), 2.03 (s, 2H), 1.97 (brs, 1H); <sup>13</sup>C NMR (125 MHz,  $\delta$ <sub>C</sub>, DMSO-*d*<sub>6</sub>): 158.8, 158.4, 150.5, 149.4, 121.2, 112.6, 56.7, 46.71; Anal. C<sub>14</sub>H<sub>17</sub>N<sub>5</sub>O<sub>3</sub>: C, 55.44; H, 5.65; N, 23.09; Found: C, 55.39; H, 5.62; N, 23.11.

**2-(2-nitrobenzyl)-N-(pyrimidin-2-yl)hydrazine-1-carboxamide (20)**

Yield: 63%; mp 239-241 °C; FT-IR (ATR,  $\nu$  cm<sup>-1</sup>): 3362 (-NH), 3219 (NHCONH), 1710 (>C=O); <sup>1</sup>H NMR (500 MHz,  $\delta$ <sub>H</sub>, DMSO-*d*<sub>6</sub>): 12.32 (brs, 1H), 10.11 (brs, 1H), 8.65-8.55 (m, 2H), 8.19-8.11 (m, 2H), 8.02-7.81 (m, 1H), 7.62-7.58 (m, 2H), 2.12 (s, 2H), 1.94 (brs, 1H); <sup>13</sup>C NMR (125 MHz,  $\delta$ <sub>C</sub>, DMSO-*d*<sub>6</sub>): 158.8, 158.5, 157.9, 148.4, 134.1, 130.9, 128.9, 126.9, 124.6, 110.7, 45.39; Anal. C<sub>12</sub>H<sub>12</sub>N<sub>6</sub>O<sub>3</sub>: C, 50.00; H, 4.20; N, 29.15; Found: C, 49.94; H, 4.23; N, 29.11.

**4.1.6 General procedure for the synthesis of compounds 21-24 and 26-35**

The appropriate substrate (**4-7** and **9-18**, 1.15-2.0 mmol) and CAT (2.0-3.0 mmol) were refluxed for 2 h in absolute ethanol. The solution was concentrated to yield an oily residue, which was mixed with ethyl acetate. The ethyl acetate layer was washed with water (2×100 ml) and passed through sodium sulfate (Na<sub>2</sub>SO<sub>4</sub>). The filtrate was concentrated *in vacuo* to obtain a crude product that was recrystallized from absolute ethanol to afford the title compounds (**21-24** and **26-35**).

#### 4.1.7 General procedure for the synthesis of compound 25

Compound **8** (0.60 mmol) and NBS (0.90 mmol) were dissolved in dry DCM (20 ml), and then DBU (0.90 mmol) was added. The reaction mixture was stirred at room temperature for 3-4 h. After completion, the reaction mixture was washed with 1 N HCl, 5% w/v sodium bicarbonate (NaHCO<sub>3</sub>) and brine. The DCM layer was concentrated *in vacuo* to give a crude product, which was recrystallized from methanol to afford **25** as a yellow solid.

#### 5-phenyl-N-(pyrimidin-2-yl)-1,3,4-oxadiazol-2-amine (21)

Yield: 61%; mp: 260-262 °C; FT-IR (ATR,  $\nu$  cm<sup>-1</sup>): 3240 (-NH), 1567 (-C=N); <sup>1</sup>H NMR (500 MHz,  $\delta_{\text{H}}$ , DMSO-*d*<sub>6</sub>): 8.62 (d, 1H, *J* = 5.0 Hz), 8.47 (d, 2H, *J* = 10.0 Hz), 7.94-7.87 (m, 2H), 7.53-7.35 (m, 3H), 7.07 (brs, 1H); <sup>13</sup>C NMR (125 MHz,  $\delta_{\text{C}}$ , DMSO-*d*<sub>6</sub>): 159.0, 158.0, 156.6, 131.7, 130.9, 129.8, 126.2, 125.7, 115.3. Anal. C<sub>12</sub>H<sub>9</sub>N<sub>5</sub>O: C, 60.25; H, 3.79; N, 29.27; Found: C, 60.29; H, 3.81; N, 29.24.

#### 5-(*p*-tolyl)-N-(pyrimidin-2-yl)-1,3,4-oxadiazol-2-amine (22)

Yield: 67%; mp: 265-267 °C; FT-IR (ATR,  $\nu$  cm<sup>-1</sup>): 3264 (-NH), 1556 (-C=N); <sup>1</sup>H NMR (500 MHz,  $\delta_{\text{H}}$ , DMSO-*d*<sub>6</sub>): 11.45 (brs, 1H), 8.61 (d, 2H, *J* = 5.0 Hz), 7.82-7.76 (m, 2H), 7.40-7.35 (m, 2H), 7.02 (brs, 1H), 2.38 (s, 3H, -CH<sub>3</sub>); <sup>13</sup>C NMR (125 MHz,  $\delta_{\text{C}}$ , DMSO-*d*<sub>6</sub>): 159.0, 158.0, 156.6, 131.7, 130.9, 129.8, 126.2, 125.7, 115.3. Anal. C<sub>13</sub>H<sub>11</sub>N<sub>5</sub>O: C, 61.65; H, 4.38; N, 27.65; Found: C, 61.57; H, 4.41; N, 27.63.

#### 5-(4-methoxyphenyl)-N-(pyrimidin-2-yl)-1,3,4-oxadiazol-2-amine (23)

Yield: 59%; mp: 247-249 °C; FT-IR (ATR,  $\nu$  cm<sup>-1</sup>): 3278 (-NH), 1563 (-C=N); <sup>1</sup>H NMR (500 MHz,  $\delta_{\text{H}}$ , DMSO-*d*<sub>6</sub>): 11.25 (brs, 1H), 8.62 (d, 2H, *J* = 4.5 Hz), 7.88 (d, 2H, *J* = 9.0 Hz), 7.14 (d, 2H, *J* = 9.0 Hz), 7.10 (t, 1H, *J* = 5.0 Hz), 3.84 (s, 3H); <sup>13</sup>C NMR (125 MHz,  $\delta_{\text{C}}$ , DMSO-*d*<sub>6</sub>): 162.09, 161.03, 159.1, 158.8, 128.1, 116.5, 115.6, 115.3, 55.9; Anal. C<sub>13</sub>H<sub>11</sub>N<sub>5</sub>O<sub>2</sub>: C, 57.99; H, 4.12; N, 26.01; Found: C, 58.04; H, 4.09; N, 25.98.

**5-(3,4-dimethoxy phenyl)-N-(pyrimidin-2-yl)-1,3,4-oxadiazol-2-amine (24)**

Yield: 67%; mp: 221-223 °C; FT-IR (ATR,  $\nu$  cm<sup>-1</sup>): 3261 (-NH), 1578 (-C=N); <sup>1</sup>H NMR (500 MHz,  $\delta_{\text{H}}$ , DMSO-*d*<sub>6</sub>): 11.25 (brs, 1H), 8.62 (d, 2H, *J* = 4.5 Hz), 7.69-7.49 (m, 3H) 7.14-7.09 (m, 1H), 3.85 (s, 6H); <sup>13</sup>C NMR (125 MHz,  $\delta_{\text{C}}$ , DMSO-*d*<sub>6</sub>): 167.4, 161.0, 159.1, 158.7, 157.3, 151.9, 149.5, 123.4, 119.8, 116.4, 115.7, 56.1; Anal. C<sub>14</sub>H<sub>13</sub>N<sub>5</sub>O<sub>3</sub>: C, 56.18; H, 4.38; N, 23.40; Found: C, 56.21; H, 4.34; N, 23.44.

**5-(3,4,5-trimethoxy phenyl)-N-(pyrimidin-2-yl)-1,3,4-oxadiazol-2-amine (25)**

Yield: 62%; mp: 209-211 °C; FT-IR (ATR,  $\nu$  cm<sup>-1</sup>): 3271 (-NH), 1582 (-C=N); <sup>1</sup>H NMR (500 MHz,  $\delta_{\text{H}}$ , DMSO-*d*<sub>6</sub>): 10.00 (brs, 1H), 8.49 (brs, 2H), 8.43 (brs, 1H), 7.42 (brs, 1H) 7.15 (t, 1H, *J* = 5.0 Hz), 3.88 (s, 3H), 3.83 (s, 6H); <sup>13</sup>C NMR (125 MHz,  $\delta_{\text{C}}$ , DMSO-*d*<sub>6</sub>): 158.7, 158.1, 153.2, 151.3, 150.7, 144.4, 129.0, 116.0, 110.8, 106.0, 103.8, 61.3, 56.6; Anal. C<sub>15</sub>H<sub>15</sub>N<sub>5</sub>O<sub>4</sub>: C, 54.71; H, 4.59; N, 21.27; Found: C, 54.71; H, 4.59; N, 21.27

**4-(5-(pyrimidin-2-ylamino)-1,3,4-oxadiazol-2-yl)phenol (26)**

Yield: 69%; mp: 217-219 °C; FT-IR (ATR,  $\nu$  cm<sup>-1</sup>): 3431 (-OH), 3256 (-NH), 1569 (-C=N); <sup>1</sup>H NMR (500 MHz,  $\delta_{\text{H}}$ , DMSO-*d*<sub>6</sub>): 11.19 (brs, 1H), 10.47 (s, 1H), 8.63 (m, 2H), 7.83-7.71 (m, 2H), 7.10-6.98 (m, 3H); <sup>13</sup>C NMR (125 MHz,  $\delta_{\text{C}}$ , DMSO-*d*<sub>6</sub>): 160.9, 159.1, 158.8, 132.0, 129.1, 128.2, 116.6, 114.8; Anal. C<sub>12</sub>H<sub>9</sub>N<sub>5</sub>O<sub>2</sub>: C, 56.47; H, 3.55; N, 27.44; Found: C, 56.51; H, 3.53; N, 27.47.

**2-(5-(pyrimidin-2-ylamino)-1,3,4-oxadiazol-2-yl)phenol (27)**

Yield: 67%; mp: 231-233 °C; FT-IR (ATR,  $\nu$  cm<sup>-1</sup>): 3422 (-OH), 3273 (-NH), 1557 (-C=N); <sup>1</sup>H NMR (500 MHz,  $\delta_{\text{H}}$ , DMSO-*d*<sub>6</sub>): 11.29 (brs, 1H), 10.21 (s, 1H), 8.63 (m, 2H), 7.27-7.01 (m, 5H); <sup>13</sup>C NMR (125 MHz,  $\delta_{\text{C}}$ , DMSO-*d*<sub>6</sub>): 160.4, 159.1, 158.6, 132.3, 129.7, 128.3, 126.0, 120.2, 115.8, 110.11; Anal. C<sub>12</sub>H<sub>9</sub>N<sub>5</sub>O<sub>2</sub>: C, 56.47; H, 3.55; N, 27.44; Found: C, 56.50; H, 3.57; N, 27.41.

**5-(naphthalen-1-yl)-N-(pyrimidin-2-yl)-1,3,4-oxadiazol-2-amine (28)**

Yield: 64%; mp: 242-244 °C; FT-IR (ATR,  $\nu$   $\text{cm}^{-1}$ ): 3253 (-NH), 1573 (-C=N);  $^1\text{H}$  NMR (500 MHz,  $\delta_{\text{H}}$ ,  $\text{DMSO-}d_6$ ): 11.51 (brs, 1H), 9.13 (d, 1H,  $J = 8.5$  Hz) 8.67 (d, 2H,  $J = 5.0$  Hz), 8.19-8.08 (m, 3H), 7.76-7.65 (m, 3H), 7.13 (t, 1H,  $J = 4.8$  Hz);  $^{13}\text{C}$  NMR (125 MHz,  $\delta_{\text{C}}$ ,  $\text{DMSO-}d_6$ ): 160.7, 159.1, 158.9, 158.5, 133.9, 132.5, 129.5, 129.3, 128.5, 127.2, 125.9, 125.8, 120.5, 115.9; Anal.  $\text{C}_{16}\text{H}_{11}\text{N}_5\text{O}$ : C, 66.43; H, 3.83; N, 24.21; Found: C, 66.39; H, 3.87; N, 24.19.

**5-(4-fluorophenyl)-N-(pyrimidin-2-yl)-1,3,4-oxadiazol-2-amine (29)**

Yield: 67%; mp: 219-221 °C; FT-IR (ATR,  $\nu$   $\text{cm}^{-1}$ ): 3278 (-NH), 1576 (-C=N);  $^1\text{H}$  NMR (500 MHz,  $\delta_{\text{H}}$ ,  $\text{DMSO-}d_6$ ): 11.39 (brs, 1H), 8.59 (d, 2H,  $J = 5.0$  Hz), 7.98 (d, 2H,  $J = 5.5$  Hz), 7.73-7.16 (m, 3H);  $^{13}\text{C}$  NMR (125 MHz,  $\delta_{\text{C}}$ ,  $\text{DMSO-}d_6$ ): 165.1, 163.2, 159.9, 158.5, 128.7, 127.2, 116.9, 115.5; Anal.  $\text{C}_{12}\text{H}_8\text{FN}_5\text{O}$ : C, 56.03; H, 3.13; N, 27.23; Found: C, 55.98; H, 3.11; N, 27.19.

**5-(4-chlorophenyl)-N-(pyrimidin-2-yl)-1,3,4-oxadiazol-2-amine (30)**

Yield: 58%; mp: 252-254 °C; FT-IR (ATR,  $\nu$   $\text{cm}^{-1}$ ): 3259 (-NH), 1572 (-C=N);  $^1\text{H}$  NMR (500 MHz,  $\delta_{\text{H}}$ ,  $\text{DMSO-}d_6$ ): 11.38 (brs, 1H), 8.53 (d, 2H,  $J = 3.0$  Hz), 7.89 (d, 2H,  $J = 7.0$  Hz), 7.44 (d, 2H,  $J = 7.5$  Hz), 6.94 (d, 1H,  $J = 4.5$  Hz);  $^{13}\text{C}$  NMR (125 MHz,  $\delta_{\text{C}}$ ,  $\text{DMSO-}d_6$ ): 159.5, 158.1, 158.5, 158.1, 136.8, 129.3, 127.6, 122.8, 115.2; Anal.  $\text{C}_{12}\text{H}_8\text{ClN}_5\text{O}$ : C, 52.66; H, 2.95; N, 25.59; Found: C, 52.64; H, 2.97; N, 25.63.

**5-(4-bromophenyl)-N-(pyrimidin-2-yl)-1,3,4-oxadiazol-2-amine (31)**

Yield: 67%; mp: 242-244 °C; FT-IR (ATR,  $\nu$   $\text{cm}^{-1}$ ): 3279 (-NH), 1556 (-C=N);  $^1\text{H}$  NMR (500 MHz,  $\delta_{\text{H}}$ ,  $\text{DMSO-}d_6$ ): 8.69-8.52 (m, 2H), 8.44 (s, 1H), 7.87-7.67 (m, 4H), 7.19-7.08 (m, 1H);  $^{13}\text{C}$  NMR (125 MHz,  $\delta_{\text{C}}$ ,  $\text{DMSO-}d_6$ ): 159.9, 159.6, 159.1, 158.7, 158.7, 156.7, 132.9, 128.1, 125.2, 123.4, 115.6; Anal.  $\text{C}_{12}\text{H}_8\text{BrN}_5\text{O}$ : C, 45.31; H, 2.53; N, 22.01; Found: C, 45.24; H, 2.51; N, 21.98

**5-(3-bromophenyl)-N-(pyrimidin-2-yl)-1,3,4-oxadiazol-2-amine (32)**

Yield: 59%; mp: 197-199 °C; FT-IR (ATR,  $\nu$  cm<sup>-1</sup>): 3264 (-NH), 1569 (-C=N); <sup>1</sup>H NMR (500 MHz,  $\delta_{\text{H}}$ , DMSO-*d*<sub>6</sub>): 8.86 (s, 1H), 8.45 (d, 2H, *J* = 5.0 Hz), 7.70 (d, 2H, *J* = 8.0 Hz), 7.17 (d, 2H, *J* = 7.5 Hz), 6.89 (t, 1H, *J* = 4.8 Hz); <sup>13</sup>C NMR (125 MHz,  $\delta_{\text{C}}$ , DMSO-*d*<sub>6</sub>): 159.5, 158.5, 156.9, 143.8, 139.9, 128.6, 127.0, 114.4; Anal. C<sub>12</sub>H<sub>8</sub>BrN<sub>5</sub>O: C, 45.31; H, 2.53; N, 22.01; Found: C, 45.27; H, 2.49; N, 22.04.

**5-(2-chlorophenyl)-N-(pyrimidin-2-yl)-1,3,4-oxadiazol-2-amine (33)**

Yield: 64%; mp: 172-174 °C; FT-IR (ATR,  $\nu$  cm<sup>-1</sup>): 3284 (-NH), 1544 (-C=N); <sup>1</sup>H NMR (500 MHz,  $\delta_{\text{H}}$ , DMSO-*d*<sub>6</sub>): 11.48 (brs, 1H), 8.55 (d, 2H, *J* = 5.0 Hz), 7.88 (d, 1H, *J* = 8.0 Hz), 7.70 (d, 1H, *J* = 8.0 Hz), 7.48 (t, 1H, *J* = 7.8 Hz), 7.43 (t, 1H, *J* = 7.8 Hz), 6.99 (t, 1H, *J* = 5.0 Hz); <sup>13</sup>C NMR (125 MHz,  $\delta_{\text{C}}$ , DMSO-*d*<sub>6</sub>): 167.3, 159.3, 158.6, 158.3, 156.8, 142.0, 141.6, 132.3, 131.3, 130.9, 129.3, 128.8, 127.5, 115.4; Anal. C<sub>12</sub>H<sub>8</sub>ClN<sub>5</sub>O: C, 52.66; H, 2.95; N, 25.59; Found: C, 52.65; H, 2.93; N, 25.76.

**5-(4-nitrophenyl)-N-(pyrimidin-2-yl)-1,3,4-oxadiazol-2-amine (34)**

Yield: 61%; mp: 263-265 °C; FT-IR (ATR,  $\nu$  cm<sup>-1</sup>): 3271 (-NH), 1550 (-C=N); <sup>1</sup>H NMR (500 MHz,  $\delta_{\text{H}}$ , DMSO-*d*<sub>6</sub>): 11.34 (brs, 1H), 8.66 (d, 2H, *J* = 4.3 Hz), 8.43 (d, 2H, *J* = 8.5 Hz), 7.70-7.69 (m, 2H), 7.15 (t, 1H, *J* = 4.5 Hz); <sup>13</sup>C NMR (125 MHz,  $\delta_{\text{C}}$ , DMSO-*d*<sub>6</sub>): 159.1, 158.2, 149.1, 132.0, 129.6, 129.1, 127.5, 125.1, 116.1; Anal. C<sub>12</sub>H<sub>8</sub>N<sub>6</sub>O<sub>3</sub>: C, 50.71; H, 2.84; N, 29.57; Found: C, 50.64; H, 2.81; N, 29.54.

**5-(2-nitrophenyl)-N-(pyrimidin-2-yl)-1,3,4-oxadiazol-2-amine (35)**

Yield: 67%; mp: 192-194 °C; FT-IR (ATR,  $\nu$  cm<sup>-1</sup>): 3274 (-NH), 1549 (-C=N); <sup>1</sup>H NMR (500 MHz,  $\delta_{\text{H}}$ , DMSO-*d*<sub>6</sub>): 11.37 (brs, 1H), 8.78 (d, 2H, *J* = 5.0 Hz), 8.11-8.01 (m, 2H), 7.80-7.74 (m, 2H), 7.08 (t, 1H, *J* = 5.0 Hz); <sup>13</sup>C NMR (125 MHz,  $\delta_{\text{C}}$ , DMSO-*d*<sub>6</sub>): 159.3, 158.8, 157.1, 156.9, 148.1, 133.0, 132.0, 131.6, 124.5, 118.7, 115.7; Anal. C<sub>12</sub>H<sub>8</sub>N<sub>6</sub>O<sub>3</sub>: C, 50.71; H, 2.84; N, 29.57; Found: C, 50.68; H, 2.87; N, 29.59.

## 4.2. Pharmacology

### 4.2.1 *In vitro* cholinesterase inhibition assay

The cholinesterase inhibitory activities of the target compounds were evaluated against human AChE following the modified Ellman's protocol.<sup>59</sup> Solutions of the test compounds were prepared in DMSO. A solution of hAChE (AChE from human erythrocytes, Sigma 3.1.1.7) at a concentration of 0.02 units/ml was prepared in 0.1 M sodium phosphate buffer containing 0.1% v/v Triton X-100 at pH 7.4. A stock solution of 0.02 units/ml hBChE (BChE from human serum, Sigma 3.1.1.8) was prepared by dissolving hBChE in an aqueous solution of 0.1% w/v gelatin at pH 7.4.

Briefly, 25  $\mu$ l of the respective enzyme (hAChE or hBChE) and 20  $\mu$ l of the solution of the test compound were incubated at 37 °C for 10 min. Then, 240  $\mu$ l of 0.1 M sodium phosphate buffer with 340  $\mu$ M 5,5'-dithiobis-2-nitrobenzoic acid (DTNB) and 550  $\mu$ M substrate (acetylthiocholine iodide (ATCI) or butyrylthiocholine iodide (BTCl)) was added. The rate of the reaction was monitored by measuring the absorbance at 412 nm at 37 °C for 10 min. The reaction rates in the presence and absence of the inhibitors were compared, and percentage inhibition was determined using the following expression: percentage inhibition (%) =  $(V_c - V_t/V_c) \times 100$ , where  $V_c$  and  $V_t$  are the reaction rates in the absence and presence of the inhibitor, respectively. Furthermore, the  $IC_{50}$  values were calculated using nonlinear regression (curve fitting) and the slope of the log [inhibitor] versus response curve using Graph Pad Prism 5.01. The determined  $IC_{50}$  values were relative, and Hill slopes were observed at more than 0.6. The final concentration of DMSO was maintained at  $\leq 1\%$  v/v, because at this concentration, it had no effect on cholinesterase activity. The  $pIC_{50}$  values were calculated using the following formula:  $[-\text{Log}(IC_{50} \times 10^{-6} \text{ M})]$ . Furthermore, the selectivity index (S.I.) corresponded to the antilog of  $\Delta pIC_{50}$ ;  $\Delta pIC_{50} = pIC_{50}$  of hAChE -  $pIC_{50}$  of hBChE.<sup>52,60,61</sup>

The type of enzyme inhibition by compound **28** was determined by the Lineweaver-Burk method using three concentrations of the test compound (0.15, 0.30 and 0.60  $\mu\text{M}$ ). Each concentration of the test compound was evaluated against five different concentrations of the substrate (acetylthiocholine iodide; 50-500  $\mu\text{M}$ ). The absorbance was recorded at 412 nm at 37 °C.<sup>62</sup>

#### **4.2.2 DPPH assay**

The DPPH assay was used to determine the antioxidant activities of the synthesized compounds, and ascorbic acid was used as the standard. Briefly, 50  $\mu\text{l}$  of a 20  $\mu\text{M}$  solution of the test compound was incubated with 150  $\mu\text{l}$  of DPPH solution (0.5 mM). The microplate was shaken for a few minutes and kept in the dark for 30 min to prevent photochemical reactions, and the absorbance at 517 nm was recorded. The antiradical activity was calculated using the following expression: percentage inhibition (%) =  $(A_o - A_i / A_o) \times 100$ , where  $A_o$  and  $A_i$  are the absorbances in the absence and presence of the inhibitor, respectively. Each experiment was carried out in triplicate.<sup>63,64</sup>

#### **4.2.3 PI displacement assay**

A propidium iodide displacement assay is useful for determining the binding of a compound to the peripheral site of AChE by competitively displacing propidium iodide. Briefly, 150  $\mu\text{l}$  of a 30  $\mu\text{M}$  solution of the test compound was incubated with 5 units of hAChE at 25 °C for 6 h. After incubation, 20  $\mu\text{l}$  of 1  $\mu\text{M}$  PI solution was added, and the fluorescence intensity was observed at an excitation wavelength ( $\lambda_{\text{ex}}$ ) of 535 nm and an emission wavelength ( $\lambda_{\text{em}}$ ) of 595 nm using a fluorescence plate reader (Synergy H1M, Biotek). The percentage inhibition was calculated using the following formula:  $(IF_c - IF_i / IF_c) \times 100$ , where  $IF_c$  and  $IF_i$  are the fluorescence intensities in the absence and presence of the test compounds, respectively, and the values are expressed as the mean  $\pm$  SD. Each experiment was carried out in triplicate.<sup>65</sup>

#### 4.2.4 PAMPA-BBB Assay

The test compounds (**25**, **26** and **28**) were assessed for their BBB permeability using the PAMPA-BBB assay. Initially, a filter membrane was coated with 4  $\mu$ l of porcine brain lipid (PBL), and 200  $\mu$ l of 7:3 phosphate-buffered saline:ethanol solution was added to the acceptor plate. Stock solutions (5 mg/ml) of the test compounds (**25**, **26** and **28**) were prepared in DMSO. Secondary stock solutions (25  $\mu$ g/ml) were prepared by diluting 10  $\mu$ l of the stock solution with 7:3 phosphate-buffered saline:ethanol solution. The secondary stock solution (200  $\mu$ l) was added into the donor microplate. The acceptor microplate was sandwiched on top of the donor plate, and the stack was incubated at 25 °C for 20 h. The concentrations of the test compounds and standard drugs were analyzed by recording the absorbances, and all analyses were conducted in triplicate.<sup>66</sup>

#### 4.2.5 Thioflavin T assay

The inhibitory activity of compound **28** against hAChE-induced  $A\beta_{1-42}$  aggregation was assessed by the ThT assay.  $A\beta_{1-42}$  was dissolved in 1% v/v ammonium hydroxide solution to obtain a 2000  $\mu$ M stock solution, and the solution was stored at -80 °C. The test compounds were dissolved in DMSO and diluted with PBS. The final concentration of DMSO was maintained at less than 1% v/v. Briefly,  $A\beta_{1-42}$  (10  $\mu$ M; 2  $\mu$ l) was incubated with hAChE (230  $\mu$ M; 16  $\mu$ l) in the presence or absence of test compound **28** (5  $\mu$ M, 10  $\mu$ M, and 20  $\mu$ M; 2  $\mu$ l) at 37 °C for 48 h. Then, ThT (180  $\mu$ l, 5  $\mu$ M) was added to the assay mixture, and the fluorescence intensities were recorded at an excitation wavelength of 485 nm and an emission wavelength of 528 nm using a fluorescence plate reader (Synergy H1M, Biotek). The percentage inhibition of hAChE-induced  $A\beta$  aggregation was calculated using the following expression:  $(IF_c - IF_i / IF_c) \times 100$ , where  $IF_c$  and  $IF_i$  are the fluorescence intensities in the absence and presence of the inhibitor, respectively. Each experiment was performed in triplicate.<sup>67</sup>

#### 4.2.6 Neurotoxicity assay

The neurotoxicity of compound **28** was evaluated against SH-SY5Y neuroblastoma cells by the MTT assay. Initially, SH-SY5Y cells (density of  $1 \times 10^5$ /well) were seeded in a 96-well cell tissue culture plate in 100  $\mu$ L of the medium and incubated for 24 h at 37 °C in a humidified atmosphere with 5% v/v carbon dioxide (CO<sub>2</sub>). The neuroblastoma cells were incubated with different concentrations of the test compound (100  $\mu$ l, 20-320  $\mu$ M) for 24 h. Then, 20  $\mu$ L of MTT (3-(4,5-dimethylthiazol-2-yl)-2,5-diphenyl tetrazolium bromide) solution (5 mg/ml) was added, and the assay mixture was further incubated at 37 °C (5% v/v CO<sub>2</sub>) for 3 h. After incubation, the formation of a purple color was observed under a microscope, and the solids in the assay mixture was solubilized by the addition of DMSO (100  $\mu$ L). The final concentration of DMSO was maintained at less than 0.1% v/v, as at this concentration, it had an insignificant influence on the neuroblastoma cells.<sup>68</sup> The absorbance was measured at 570 nm using the microplate reader (Synergy H1M, BioTek). The percentages of cell viability were calculated and compared to that of the control. The IC<sub>50</sub> values were determined using a nonlinear regression (curve fitting) and the slope of the log [inhibitor] versus variable response curves with Graph Pad Prism 5.01.

#### 4.2.7 *In vivo* studies

##### 4.2.7.1 Animals

*In vivo* studies were performed on adult male Swiss albino mice (25-30 g), which were purchased from Central Animal Breeding House, Institute of Medical Sciences (IMS), Banaras Hindu University (BHU), Varanasi, India. The animals were kept in groups of six per polyacrylic cage and were given semisynthetic balanced diet and water *ad libitum*. The animals were kept at a temperature of  $25 \pm 2$  °C with a relative humidity of  $55 \pm 10\%$  under 12 h light/dark cycles. Different animals were used for each behavioral investigation. The

study protocols were approved by the institutional animal ethics committee (No. Dean/2017/CAEC/94).

#### *4.2.7.2 Acute oral toxicity study*

The acute oral toxicity of compound **28** was evaluated on healthy Swiss albino mice as per the OECD-423, 2001 guidelines. The test compound was administered at various doses up to 500 mg/kg p.o., and the animals were observed at 30 min, 2 h, 4 h and 24 h to determine changes in their autonomic and behavioral responses. The animals were also observed for tremors, convulsions, salivation, diarrhea, lethargy, sleep and coma for 14 days.<sup>54</sup>

#### *4.2.7.3 Materials*

Scopolamine hydrobromide was purchased from Sigma-Aldrich, India. The experiments were performed on a Y-Maze and two-compartment passive avoidance apparatus.

#### *4.2.7.4 Experimental strategy and drug administration protocol*

The test compound was suspended in 0.3% w/v sodium carboxymethylcellulose (CMC). The behavioral studies were performed in seven groups, with each group having six mice as follows: (i) control, (ii) scopolamine hydrobromide (0.5 mg/kg, i.p.), (iii) vehicle + scopolamine, (iv) donepezil (5 mg/kg, p.o.) + scopolamine, (v) compound **28** (2.5 mg/kg, p.o.) + scopolamine, (vi) compound **28** (5 mg/kg, p.o.) + scopolamine, and (vii) compound **28** (10 mg/kg, p.o.) + scopolamine. Treatments were administered once daily for seven consecutive days to the respective group of animals. Scopolamine hydrobromide was dissolved in distilled water and administered intraperitoneally to the mice 30 min after the drug treatment on the 7<sup>th</sup> day of the experiment.

#### *4.2.7.5 Y-maze Test*

The Y-maze apparatus consists of a three-arm maze and is mostly used for the assessment of instant and short working memory in rodents. On the 7<sup>th</sup> day of treatment, 30 min after administration of the test compound, scopolamine hydrobromide was administered

intraperitoneally to all the groups except the control. Each mouse was kept at the center of the maze and allowed to explore all three arms. The total arm entries and spontaneous alterations were observed over a period of 5 min. The "memory improvement score" was calculated as % spontaneous alteration rate = (Number of alterations/(total arm entries – 2)) x 100.<sup>69</sup>

#### *4.2.7.6 Passive avoidance experiment*

The passive avoidance apparatus is a fabricated box with two compartments (dark/lit; each region is 12 × 10 × 12 cm) connected through a door, and a stainless steel electric bar (2 mm) is placed at a distance of 0.5 cm. The instrument has an electronic display timer and voltage system to regulate current flow (0.05 mA) and voltage (20 V). The experiment was performed in two separate tests: an acquisition and a retention test. The interval between the acquisition and retention tests was one day. Both tests were performed for a total period of 300 seconds. The treatment was given once daily for seven days to the animals in the respective groups. The experiment was performed on the 7<sup>th</sup> day of dosing. The acquisition test was initiated after intraperitoneal administration of scopolamine hydrobromide. After five minutes, each mouse was kept in the lit chamber of the two-compartment apparatus for 30 seconds (acquisition time). The entry door of the second dark compartment was opened, and following the entry of the mouse into the dark compartment, the door was locked. Next, a medium intensity electric shock (0.05 mA, 2 seconds) was applied to the foot through the stainless steel electric bar. The next day, the retention test was performed in which each mouse was kept in the lit chamber and observed for entry from the lit to the dark chamber within 300 seconds. Entry into the dark chamber was measured as the transfer latency time (TLT). To prevent reacquisition, no foot shock was delivered in the retention test.<sup>70</sup>

#### *4.2.8 Dissection and homogenization*

After completion of the behavioral assessments, mice were sacrificed through cervical dislocation. The whole brain was isolated, washed with cold double distilled water and with

precooled normal saline. Each whole brain was homogenized with 3 ml of 10 mM phosphate-buffered saline (pH 7.4) in a Teflon-glass homogenizer with an ice-cold bath and centrifuged at 8050  $\times$ g for 10 min at 4 °C.

#### **4.2.9 Lowry method for protein estimation**

An alkaline copper solution was prepared following the previously reported procedure from Lowry et al. The supernatant (0.2 ml) of each brain homogenate was mixed with the alkaline copper solution (1 ml) in a test tube and incubated at room temperature for 10 min. Then, 0.1 ml of phenol reagent (Folin and Ciocalteu) was quickly added. After 30 min, the absorbance was measured at a wavelength of 750 nm. The standard curve of the absorbance versus protein concentration was plotted to calculate the protein content (per mg) of the sample.<sup>71</sup>

#### **4.2.10 Ex vivo estimation of AChE**

An *ex vivo* study was performed using Ellman's method to determine the brain AChE inhibitory activity of compound **28**. Briefly, 25  $\mu$ l of brain supernatant, 150  $\mu$ l of 0.1 M sodium phosphate buffer (pH 7.4) and 100  $\mu$ l of 1 mM DTNB were added to 96-well microplates. The assay mixture was incubated for 10 min at 37 °C, and then 20  $\mu$ l of 7.5 mM ATCI was added. The rate of hydrolysis was measured at a wavelength of 412 nm for 10 min. The results are expressed as ACh hydrolyzed/min/mg protein.<sup>7</sup>

#### **4.2.11 Biochemical estimation of the oxidative stress factors**

##### **4.2.11.1 2-Thiobarbituric acid reactive substances (TBARS) estimation**

MDA was estimated using the thiobarbituric acid reactive substance (TBARS) method. The supernatant was incubated with an equal amount of 0.1 M phosphate buffer (pH 7.4) at 37 °C for 2 h. Then, 10% w/v cold trichloroacetic acid solution was added into the assay mixture, and the mixture was then centrifuged at 1006  $\times$ g for 5 min. After centrifugation, 100  $\mu$ l of the supernatant and 100  $\mu$ l of 0.67% w/v 2-sulfanylidene-1,3-diazinane-4,6-dione (2-thiobarbituric acid) were mixed. The mixture was heated at 50 °C for 10 min, cooled and then

combined with 100  $\mu$ l of double distilled water. The absorbance was measured at a wavelength of 532 nm. The MDA content was calculated from the standard curve and is expressed as the number of moles of MDA/mg of protein.<sup>72</sup>

#### 4.2.11.2 Estimation of the total nonprotein thiol

The method reported by Sedlak and Lindsay was used to determine the total nonprotein thiol content in the brain samples.<sup>57</sup> Prior to the assay, all the solutions were prepared in Tris-EDTA buffers (0.4 M Tris buffer; 0.02 M Na<sub>2</sub>EDTA; pH 8.9) and deoxygenated for 2-3 min with nitrogen. Initially, 1.0 ml of the supernatant and 1.0 ml of 5% w/v TCA solution containing Tris-EDTA buffer were mixed and centrifuged for 10-15 min at 3000  $\times$ g. After centrifugation, 50  $\mu$ l of the supernatant from the TCA precipitation and 200  $\mu$ l of Tris buffer (0.4 M; 0.02 M Na<sub>2</sub>EDTA; pH 8.9) were mixed, and then 20  $\mu$ l of 0.01 M DTNB was added. The absorbance was recorded within 5 min of the addition of DTNB at 412 nm against a reagent blank with no supernatant to determine the rate (change in absorbance/min) of formation of the colored product (2-nitro-5-thiobenzoic acid). The total nonprotein thiol content was calculated and is expressed as  $\mu$ M/mg of protein.

#### 4.2.11.3 Superoxide dismutase (SOD) assay

The reagent was prepared by mixing 0.1 mM ethylenediaminetetraacetic acid (EDTA), 24  $\mu$ M nitro blue tetrazolium (NBT), and 50 mM anhydrous sodium carbonate (Na<sub>2</sub>CO<sub>3</sub>). Then, 200  $\mu$ l of the prepared reagent was mixed with 50  $\mu$ l of the supernatant and 50  $\mu$ l of hydroxylamine hydrochloride (NH<sub>2</sub>OH.HCl). The pH of the assay mixture was maintained at 10.2, and the absorbance was recorded at 560 nm.<sup>73</sup>

#### 4.2.12 Statistical analyses

The *in vitro* results of cholinesterase inhibition, DPPH scavenging, PI displacement, PAMPA-BBB, hAChE-induced A $\beta$  aggregation inhibition, and neurotoxicity assays are expressed as the mean  $\pm$  S.D. (n = 3). The results of the *in vivo*, *ex vivo* and biochemical

analyses were analyzed by one-way analysis of variance (ANOVA) followed by Tukey's test or two-way ANOVA followed by Bonferroni's multiple comparison test, and the values are expressed as the mean  $\pm$  S.D. ( $n = 6$ ). Graph Pad Prism 5.01 was used for all statistical analyses.

### 4.3. Computational Studies

#### 4.3.1. *In silico docking simulations*

Molecular docking studies were carried out to analyze the binding behavior and active site interactions between compound **28** and hAChE (PDB Code: 4EY7).<sup>74</sup> The crystal structure of the protein was prepared using the Protein Preparation Wizard module in Schrödinger 2018-1. Initially, hydrogens were added, and the partial charges were assigned using the OPLS-2005 force field. The missing side chains and loops were added using Prime. All the water molecules were deleted, and the protonation states were assigned using Epik at pH  $7.0 \pm 2.0$ . Then, the protein structure was optimized by the PROPKA method at pH 7.0 and minimized with restrained minimization by keeping the RMSD of the convergence heavy atoms to 0.30 Å. The prepared protein structure was used for receptor grid generation to identify the active sites within a distance of  $10 \times 10 \times 10$  Å from the centroid of the cocrystallized ligand (donepezil). The LigPrep module was used to generate the stable conformers of the ligands (compound **28** and donepezil), which were docked using the Glide XP module of Schrödinger Maestro 2018-1. The detailed analyses of the interactions were performed using the Glide XP Visualizer tool.

#### 4.3.2. *Molecular Dynamics*

A molecular dynamics simulation run of 30 nsec was performed to confirm the binding stability and pattern of the compound **28**-hAChE complex using Desmond. Initially, the system was built using the system builder in which a virtual water environment was created by a cubic simulation box of the TIP3P explicit water system with a minimum distance of 10

Å between the box wall and the protein-ligand complex. Counterions were added to neutralize the system, and 0.15 M NaCl was added to maintain the isosmotic salt environment. A conjugate gradient algorithm with a maximum of 2000 interactions with convergence criteria of 1 kcal/mol/Å was used for the energy minimization of the system. After energy minimization, a simulation run of 30 nsec was performed with periodic boundary conditions under isothermal-isobaric ensemble (NPT).

### CONFLICT OF INTEREST

The authors declare no conflict of interest.

### ACKNOWLEDGMENTS

The authors gratefully acknowledge the Central Instrument Facility (CIF), Indian Institute of Technology (Banaras Hindu University), Varanasi, for conducting the NMR experiments. We are also thankful to the Department of Health Research, Ministry of Health and Family Welfare for providing a Young Scientist Grant in newer areas of Drugs Chemistry (25011/215-HRD/2016-HR).

### SUPPLEMENTARY INFORMATION

The results of the computational studies and the  $^1\text{H}$  NMR and  $^{13}\text{C}$  NMR spectra of the synthesized compounds.

### REFERENCES

1. Geronikaki AA, Dearden JC, Filimonov D, Galaeva I, Garibova TL, Glorizova T, Krajneva V, Lagunin A, Macaev FZ, Molodavkin G. *J Med Chem.* **2004**;47(11): 2870-2876.
2. Piplani P, Danta CC. *Bioorg Chem.* **2015**;60: 64-73.
3. Guillozet AL, Weintraub S, Mash DC, Mesulam MM. *Arch Neurol.* **2003**;60(5): 729-736.
4. Tham W, Auchus AP, Thong M, Goh M-L, Chang H-M, Wong M-C, Chen CP-H. *J Neurol Sci.* **2002**;203: 49-52.
5. Tyler CR, Allan AM. *Curr Environ Health Rep.* **2014**;1(2): 132-147.

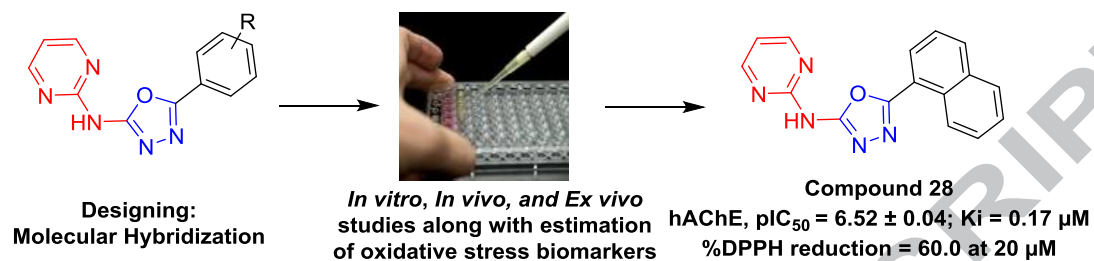
6. Guskiewicz KM, Marshall SW, Bailes J, McCrea M, Cantu RC, Randolph C, Jordan BD. *Neurosurgery*. **2005**;57(4): 719-726.
7. Tripathi PN, Srivastava P, Sharma P, Tripathi MK, Seth A, Tripathi A, Rai SN, Singh SP, Shrivastava SK. *Bioorg Chem*. **2019**;85: 82-96.
8. Srivastava P, Tripathi PN, Sharma P, Rai SN, Singh SP, Srivastava RK, Shankar S, Shrivastava SK. *Eur J Med Chem*. **2019**;163: 116-135.
9. Etcheberrigaray R, Alkon DL: **Methods for Alzheimer's Disease treatment and cognitive enhancement**. In: *United States Patent*. Edited by Patent U. USA: Blanchette Rockefeller Neurosciences Institute, Morgantown, WV; 2004.
10. Shrivastava SK, Sinha SK, Srivastava P, Tripathi PN, Sharma P, Tripathi MK, Tripathi A, Choubey PK, Waiker DK, Aggarwal LM. *Bioorg Chem*. **2018**;82: 211-223.
11. Blokland A. *Brain Research Reviews*. **1995**;21(3): 285-300.
12. Kulisevsky J. *Drugs Aging*. **2000**;16(5): 365-379.
13. Sirviö J, Riekkinen Jr P, Jäkälä P, Riekkinen PJ. *Prog Neurobiol*. **1994**;43(4-5): 363-379.
14. Vogel W, Broverman DM, Draguns JG, Klaiber EL. *Psychol Bull*. **1966**;65(6): 367.
15. Sharma P, Srivastava P, Seth A, Tripathi PN, Banerjee AG, Shrivastava SK. *Prog Neurobiol*. **2019**;174: 53-89.
16. Horel JA. *Brain*. **1978**;101(4): NP1-NP1.
17. Easton A, Douchamps V, Eacott M, Lever C. *Neuropsychologia*. **2012**;50(13): 3156-3168.
18. Johnson G, Moore S. *Curr Pharm Des*. **2006**;12(2): 217-225.
19. De Ferrari GV, Canales MA, Shin I, Weiner LM, Silman I, Inestrosa NC. *Biochemistry*. **2001**;40(35): 10447-10457.
20. Jomova K, Vondrakova D, Lawson M, Valko M. *Mol Cell Biochem*. **2010**;345(1-2): 91-104.
21. Liu R, Liu IY, Bi X, Thompson RF, Doctrow SR, Malfroy B, Baudry M. *Proceedings of the National Academy of Sciences*. **2003**;100(14): 8526-8531.
22. Markesbery WR. *Free Radic Biol Med*. **1997**;23(1): 134-147.
23. Peauger L, Azzouz R, Gembus V, Tintas M-L, Sopková-de Oliveira Santos J, Bohn P, Papamicaël C, Levacher V. *J Med Chem*. **2017**;60(13): 5909-5926.
24. Thompson S, Lanctôt KL, Herrmann N. *Expert opinion on drug safety*. **2004**;3(5): 425-440.

25. Ali TB, Schleret TR, Reilly BM, Chen WY, Abagyan R. *PLoS One*. **2015**;10(12): e0144337.
26. Sharma P, Tripathi A, Tripathi PN, Prajapati SK, Seth A, Tripathi MK, Srivastava P, Tiwari V, Krishnamurthy S, Shrivastava SK. *Eur J Med Chem*. **2019**: DOI: <https://doi.org/10.1016/j.ejmech.2019.1002.1030>.
27. Svetlik J, Veizerová L, Mayer TU, Catarinella M. *Bioorg Med Chem Lett*. **2010**;20(14): 4073-4076.
28. Luthra PM, Mishra CB, Jha PK, Barodia SK. *Bioorg Med Chem Lett*. **2010**;20(3): 1214-1218.
29. Hu J, Wang Y, Wei X, Wu X, Chen G, Cao G, Shen X, Zhang X, Tang Q, Liang G. *Eur J Med Chem*. **2013**;64: 292-301.
30. Fatima S, Sharma A, Saxena R, Tripathi R, Shukla SK, Pandey SK, Tripathi R, Tripathi RP. *Eur J Med Chem*. **2012**;55: 195-204.
31. Figueiredo J, Ismael M, Pinheiro J, Silva A, Justino J, Silva F, Goulart M, Mira D, Araújo M, Campoy R. *Carbohydr Res*. **2012**;347(1): 47-54.
32. Basiri A, Murugaiyah V, Osman H, Kumar RS, Kia Y, Hooda A, Parsons RB. *Biorg Med Chem*. **2014**;22(2): 906-916.
33. Kumar J, Gill A, Shaikh M, Singh A, Shandilya A, Jameel E, Sharma N, Mrinal N, Hoda N, Jayaram B. *ChemistrySelect*. **2018**;3(2): 736-747.
34. Valasani KR, Chaney MO, Day VW, ShiDu Yan S. *Journal of chemical information and modeling*. **2013**;53(8): 2033-2046.
35. Kumar J, Meena P, Singh A, Jameel E, Maqbool M, Mobashir M, Shandilya A, Tiwari M, Hoda N, Jayaram B. *Eur J Med Chem*. **2016**;119: 260-277.
36. Kumar B, Dwivedi AR, Sarkar B, Gupta SK, Krishnamurthy S, Mantha AK, Parkash J, Kumar V. *ACS Chem Neurosci*. **2018**.
37. Mohamed T, Rao PP. *Bioorg Med Chem Lett*. **2010**;20(12): 3606-3609.
38. Mohamed T, Yeung JC, Rao PP. *Bioorg Med Chem Lett*. **2011**;21(19): 5881-5887.
39. Mohamed T, Yeung JC, Vasefi MS, Beazely MA, Rao PP. *Bioorg Med Chem Lett*. **2012**;22(14): 4707-4712.
40. Mohamed T, Zhao X, Habib LK, Yang J, Rao PP. *Biorg Med Chem*. **2011**;19(7): 2269-2281.
41. Gurjar AS, Darekar MN, Yeong KY, Ooi L. *Biorg Med Chem*. **2018**;26(8): 1511-1522.

42. Makhaeva GF, Lushchekina SV, Boltneva NP, Serebryakova OG, Rudakova EV, Ustyugov AA, Bachurin SO, Shchepochkin AV, Chupakhin ON, Charushin VN. *Biorg Med Chem.* **2017**;25(21): 5981-5994.
43. Wang J, Cai P, Yang X-L, Li F, Wu J-J, Kong L-Y, Wang X-B. *Eur J Med Chem.* **2017**;139: 68-83.
44. Banerjee AG, Das N, Shengule SA, Sharma PA, Srivastava RS, Shrivastava SK. *Bioorg Chem.* **2016**;69: 102-120.
45. Banerjee AG, Das N, Shengule SA, Srivastava RS, Shrivastava SK. *Eur J Med Chem.* **2015**;101: 81-95.
46. Boström J, Hogner A, Llinàs A, Wellner E, Plowright AT. *J Med Chem.* **2012**;55(5): 1817-1830.
47. Kamal A, Shaik AB, Reddy GN, Kumar CG, Joseph J, Kumar GB, Purushotham U, Sastry GN. *Med Chem Res.* **2014**;23(4): 2080-2092.
48. Rehman A-u, Nafeesa K, Abbasi MA, Siddiqui SZ, Rasool S, Shah SAA, Ashraf M. *Cogent Chemistry.* **2018**;4(1): 1472197.
49. Mei W-w, Ji S-s, Xiao W, Wang X-d, Jiang C-s, Ma W-q, Zhang H-y, Gong J-x, Guo Y-w. *Monatshefte für Chemie-Chemical Monthly.* **2017**;148(10): 1807-1815.
50. Mukherjee S, Tripathi PN, Mandal SB. *Org Lett.* **2012**;14(16): 4186-4189.
51. Shrivastava SK, Srivastava P, Bandresh R, Tripathi PN, Tripathi A. *Biorg Med Chem.* **2017**;25(16): 4424-4432.
52. Tumiatti V, Milelli A, Minarini A, Rosini M, Bolognesi ML, Micco M, Andrisano V, Bartolini M, Mancini F, Recanatini M. *J Med Chem.* **2008**;51(22): 7308-7312.
53. Agholme L, Lindström T, Kågedal K, Marcusson J, Hallbeck M. *J Alzheimers Dis.* **2010**;20(4): 1069-1082.
54. Seth A, Sharma PA, Tripathi A, Choubey PK, Srivastava P, Tripathi PN, Shrivastava SK. *Med Chem Res.* **2018**;27(4): 1206-1225.
55. Klinkenberg I, Blokland A. *Neurosci Biobehav Rev.* **2010**;34(8): 1307-1350.
56. Jayakumar T, Thomas PA, Geraldine P. *Exp Gerontol.* **2007**;42(3): 183-191.
57. Sedlak J, Lindsay RH. *Anal Biochem.* **1968**;25: 192-205.
58. Toniazzo AP, Arcego DM, Lazzaretti C, Mota C, Schnorr CE, Pettenuzzo LF, Krolow R, Moreira JCF, Dalmaz C. *Neurochem Int.* **2019**.
59. Ellman GL, Courtney KD, Andres Jr V, Featherstone RM. *Biochem Pharmacol.* **1961**;7(2): 88-95.

60. Bolognesi ML, Cavalli A, Valgimigli L, Bartolini M, Rosini M, Andrisano V, Recanatini M, Melchiorre C. *J Med Chem.* **2007**;50(26): 6446-6449.
61. Gupta VK, Pal R, Siddiqi NJ, Sharma B. *Enzyme research.* **2015**;2015.
62. Lineweaver H, Burk D. *J Am Chem Soc.* **1934**;56(3): 658-666.
63. Brand-Williams W, Cuvelier M-E, Berset C. *LWT-Food science and Technology.* **1995**;28(1): 25-30.
64. Bondet V, Brand-Williams W, Berset C. *LWT-Food Science and Technology.* **1997**;30(6): 609-615.
65. Taylor P, Lappi S. *Biochemistry.* **1975**;14(9): 1989-1997.
66. Di L, Kerns EH, Fan K, McConnell OJ, Carter GT. *Eur J Med Chem.* **2003**;38(3): 223-232.
67. LeVine III H: **Quantification of  $\beta$ -sheet amyloid fibril structures with thioflavin T.** In: *Methods Enzymol. Volume 309*, edn.: Elsevier; 1999: 274-284.
68. Tang Y, Donnelly K, Tiffany-Castiglioni E, Mumtaz M. *Journal of Toxicology and Environmental Health Part A.* **2003**;66(10): 919-940.
69. Shidore M, Machhi J, Shingala K, Murumkar P, Sharma MK, Agrawal N, Tripathi A, Parikh Z, Pillai P, Yadav MR. *J Med Chem.* **2016**;59(12): 5823-5846.
70. Kumar D, Gupta SK, Ganeshpurkar A, Gutti G, Krishnamurthy S, Modi G, Singh SK. *Eur J Med Chem.* **2018**;150: 87-101.
71. Lowry OH, Rosebrough NJ, Farr AL, Randall RJ. *J Biol Chem.* **1951**;193(1): 265-275.
72. Wills E. *Biochem J.* **1966**;99(3): 667.
73. Kono Y. *Arch Biochem Biophys.* **1978**;186(1): 189-195.
74. Cheung J, Rudolph MJ, Burshteyn F, Cassidy MS, Gary EN, Love J, Franklin MC, Height JJ. *J Med Chem.* **2012**;55(22): 10282-10286.

## Graphical Abstract



ACCEPTED MANUSCRIPT